Effect of Preform Fibre Distribution on the Surface Finish of Composite Panels

By

Ronald Lawand

Department of Mechanical Engineering

McGill University

Montréal, Canada

A thesis submitted to

McGill University

in partial fulfillment of the requirements for the degree of

Master of Engineering

August 2009

Abstract

Achievement of high class surface finish is important to the high volume automotive industry when using the Resin Transfer Molding (RTM) process for exterior body panels. In this work, the effect of the fibre distribution in F3P preforms on the surface quality of RTM moulded panels was investigated. Taguchi experimental design techniques were employed to design test matrices and an optimization analysis was performed on the fibre preform architecture. The F3P preform fibre distribution was measured by carrying out image analysis of the light intensity transmitted through dry preforms. Test panels were manufactured using a flat plate steel mould mounted on a press. The panel surface quality was measured using the ONDULO non-contact surface measurement system. Fibre density distribution was compared to the measured surface roughness. Predicted surface quality is presented and compared to measured values from the manufactured parts. The results obtained indicate that small variations in preform fibre volume fraction and top veil thickness have no effect on the surface finish of 'Class A' composites parts.

Résumé

Dans l'industrie automobile à haut taux de production, l'obtention d'un excellent fini de surface pour les panneaux extérieurs de carrosserie, fabriqués par le procédé d'injection sur renforts est très important. Dans ce travail, l'effet de la distribution des fibres de préformes F3P sur la qualité de panneaux moulés par le procédé d'injection sur renforts a été étudié. Un plan d'expérience basé sur la méthode de Taguchi a été employé pour concevoir la matrice de tests. L'architecture de la préforme a été aussi optimisée. La distribution des fibres des préformes F3P a été mesurée en performant une analyse d'image sur l'intensité lumineuse transmise à travers la préforme sèche. Des panneaux tests ont été fabriqués sur un moule d'acier monté sur une presse. La qualité de la surface des panneaux a été mesurée par un système de mesure sans contact appelé ONDULO. La distribution de la densité de fibre a été comparée à la mesure de rugosité des surfaces. La prédiction de la qualité des surfaces est présentée et comparée aux valeurs mesurées des panneaux tests. Les résultats obtenus indiquent qu'une petite variation de la fraction volumique de fibre ainsi que de l'épaisseur du voile supérieur n'a pas d'influence sur le fini de surface type A, de pièces composites.

Acknowledgements

I would first of all like to acknowledge my supervisor, Prof. Pascal Hubert. I am honoured to have worked with you and forever grateful for the opportunities you provided me.

I would also like to acknowledge the financial support of the Auto21 Network Centres of Excellence, without whom this work wouldn't have been completed. I would also like to express my appreciation towards Dr. Ken Kendall of Aston Martin, as well as Louis Rouyez and Cédric Leray of Sotira Composites for their generous input of knowledge and materials. A big thank you goes out to Edith Roland Fotsing of École Polytechnique de Montréal for his patience working with the ONDULO system.

On a personal note, I would like to thank my dear friends in the McGill Structures and Composite Materials Laboratory, especially Jonathan Laliberté and Geneviève Palardy, for their help, guidance and most importantly friendship throughout this research. Further, I would like to express my gratitude towards Prof. Larry Lessard for his mentorship throughout my career at McGill.

Last, but not least, I would like to thank my family for their infinite love and support. I will forever strive to make you as happy as you all make me.

Table of Contents

List of Figures

List of Tables

List of Acronyms and Symbols

Acronyms

ACC	Automotive Composites Consortium
ANOVA	Analysis of Variance
DAQ	Data Acquisition System
DOE	Design of Experiments
DOI	Distinctness-of-Image
DSC	Differential Scanning Calorimeter
F3P	Ford Programmable Preforming Process
LPA	Low Profile Additives
MSD	Mean-Squared Deviation
P4	Programmable Powdered Preforming Process
PMMA	Polymethyl Methacrylate
PVAc	Polyvinyl Acetate
RTM	Resin Transfer Moulding
SMC	Sheet Moulding Compound
UP	Unsaturated Polyester

Symbols

G_a	Average Grayscale Roughness
R_a	Average Roughness
V_f	Fibre volume fraction, measured for cured part
wt%	Percent fraction of weight

1 Introduction

Improving the surface finish of composite parts manufactured by Resin Transfer Moulding (RTM) is an important step towards full-scale implementation of such components in 'Class A' automotive applications. Although composite materials are already being used in the automotive industry, research towards fulfilling the promise of strong, light weight, high-production parts continues. To place the current work in context, a glimpse at several past developments in composite materials for the automotive industry will be presented in Section 1.1. Next, the RTM process and the Ford Programmable Preforming Process (F3P) will be introduced in Sections 1.2 and 1.3 respectively. Finally, the motivation and objectives of this project will be outlined in Sections 1.4 and 1.5.

1.1 A Look at the Past

The use of composites materials is not entirely new to the automotive industry. Reaching back all the way to the late 1930s, the notion of replacing steel with more lightweight alternatives existed. It was Henry Ford who made the first efforts in the field with the introduction of a soy-based wood composite automobile body, shown in Figure 1.1 [1].

Figure 1.1: Photo of Henry Ford demonstrating the strength of his soy-based wood composite car body by taking an axe to it.

The next jump in interest towards the use of fibre-reinforced components occurred in the mid 1950s, when General Motors produced the Corvette, soon followed by low-volume Singer Hunter and Kaiser-Darrin. These initiatives were thanks to the growing commercial availability of cold setting polyester resins and glass fibre reinforcements, and were an example of the desire to produce lighter car bodies that required less costly tooling. The downside, however, was that the concept was limited to low-volume applications due to the slow processing cycle.

By the mid 1970s, both the use of reinforced and non-reinforced plastics in automobiles had grown tremendously, going in a decade from on average 11 kg to 45 kg worth of components. This growth was encouraged by the establishment of the Corporate Average Fuel Economy (CAFE) standards for passenger cars in the United States, which led to the further application of aluminum, plastics and composites in the automotive industry [2].

Currently, the use of composite materials in automotive parts is quite common. The manufacture of both structural and non-structural components has been achieved by a number of carmakers, with the processing method of choice being the Sheet Moulding Compound (SMC) technique. Recently, research seeking to implement Resin Transfer Moulding (RTM) has gained a great deal of traction. The application of new fibreglass preforming techniques in conjunction with RTM has allowed Aston Martin to produce nearly 50 000 composite components per year for its DB9 Coupe, DB9 Volante (convertible), V8 Vantage (pictured in Figure 1.2) and V8 Roadster models [3].

Figure 1.2: Photo of Aston Martin V8 Vantage, featuring fibreglass reinforced composite materials

1.2 Resin Transfer Moulding

Resin Transfer Moulding (RTM) is a process whereby dry fibrous reinforcements are infiltrated with resin and cured in a closed mould. It has garnered a great deal of attention in the automotive industry thanks to the prospect of reduced

production costs, greater thickness control and part volume fraction, as well as the ability to mould complex parts and have good surface finish on both sides [4].

The process is carried out in several steps, as described in Figure 1.3. First, a preform (a), consisting of dry fibres placed according to their desired final layup is prepared. It is then placed into a closed cavity mould (b), which has been prepared with a release agent that allows for the easy removal of the cured part. Next, resin is pumped into the mould (c) through an injection port and continues to flow until the entire cavity has been filled and the excess comes out the exit. Heat and pressure is applied (d) to cure the resin, in a manner such that the resin does not gel before the mould cavity is filled. Upon completion (e), the mould cavity is re-opened and the finished part is removed.

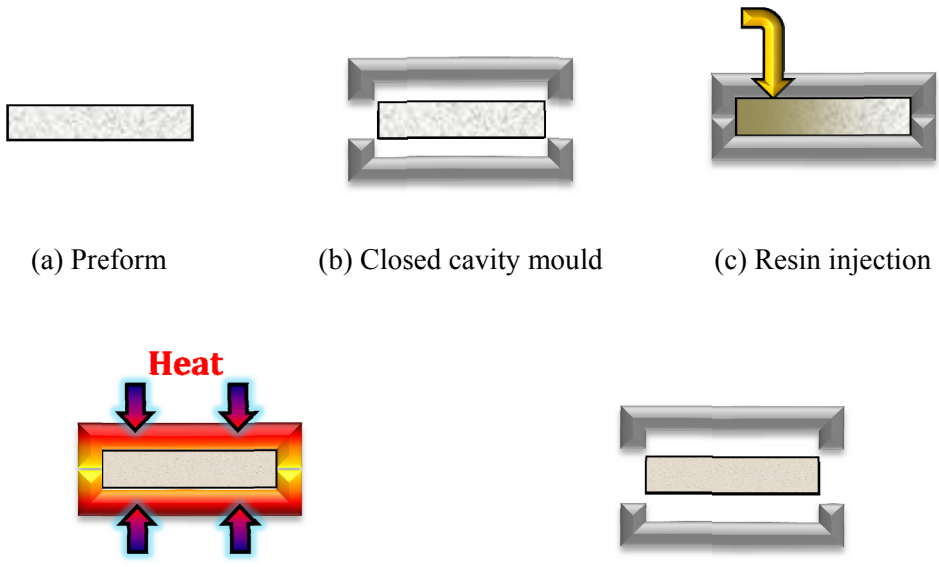

Figure 1.3: Diagram illustrating the RTM process

In the automotive industry, the process is setup such that minimal time is lost between injection runs. Preforms are prepared outside the mould, and unsaturated polyester (UP) resins are commonly used because they tend to cost less, cure more quickly and require lower curing temperatures. The UP resin mixture can also be manipulated with styrene – to control viscosity, and thermoplastic particles known as Low Profile Additives (LPA) – to control volumetric shrinkage during polymerization [5].

1.3 Ford Programmable Preforming Process

The Ford Programmable Preforming Process (F3P) is an automated preforming technique created by the Ford Motor Co. (Dearborn, MI) in cooperation with Sotira Composites (Saint Méloir des Ondes, France) and Aston Martin (Gaydon, Warwick, U.K.). The result of more than a decade of development, the process is designed to improve preforming efficiency by implementing a robotic system that reduces scrap and increases production towards high-volume applications [3]. Currently, Aston Martin depends on the combination of F3P and RTM for the production of nearly 50 000 composite components annually. Displayed in Figure 1.4 is the spraying of chopped fibres onto a component screen.

Figure 1.4: F3P System at Sotira Composites [3]

The preforming is accomplished in two stages. First, a six-axis articulated arm robot precisely sprays the chopped fibreglass onto a screen shaped in the form of the desired part. Then, hot and cold forced air is used to heat the commingled binder, thus consolidating the part, and thereafter cool the preform so it can be removed. The system at Sotira Composites has two cells which the robot arm can shuttle between, allowing preforming to be carried out in parallel – further improving the production rate.

1.4 Motivation

The automotive industry is constantly looking to improve their products, and thus reducing car weight and improving fuel efficiency are always of importance. The use of composite materials provides a great number of benefits, such as weight and tooling cost reduction as compared to equivalent metal stamped parts.

Additionally, the combination of RTM and F3P allows for improved production rates, as well as reduced labour needs and scraped material when compared to other industrial composite processing methods, such as the most commonly used Sheet Moulding Compound (SMC) [6].

A major concern during the manufacture of composite components by RTM is the surface finish quality. Parts meant to be placed on the exterior or visible to car owners are referred to as 'Class A' in the automotive industry. Each manufacturer sets their own metrics for qualifying surface finish, but generally, components should be free of any noticeable undulations and have an aesthetically pleasing shine or lustre.

The main factors contributing to the quality of the surface finish of composite components manufactured by RTM are resin volumetric changes, fibre characteristics, flow distribution and surface finish of the mould. Work has previously been carried out to study the optimal resin characteristics and RTM processing parameters. However, to this point, little is known concerning the sensitivity of a component's surface finish to variations in fibre architecture. Material selection, F3P machine parameters and fibre orientation/distribution are elements key to fibre preform quality. Thus, in order to obtain a comprehensive understanding of the material and processing parameters affecting surface finish in composite components manufactured by RTM, the effect of fibrous reinforcements must be investigated.

1.5 Work objectives and thesis outline

The objective of the current work is to understand the effect varying the architecture of fibreglass preforms prepared using the Ford Programmable Preforming Process has on the surface finish quality of composite panels manufactured by RTM. Parameters determined to be 'optimal' in previous work using the same resin system and moulding apparatus will be maintained. Research will be accomplished first by identifying the F3P preform characteristics, then by investigating preform variability, before finally attempting to relate these results to surface finish.

Chapter 2 will include background information regarding RTM, F3P, the Taguchi method, surface finish characterisation and preform imaging, as well as insightful examples of each in literature. The experimental techniques utilised in this project will be presented in Chapter 3, which will contain details concerning the Taguchi method, dry preform imaging, RTM processing, and roughness measurements. In addition to the presentation of results, Chapter 4 will contain discussion regarding the outcomes, before final conclusions are established in Chapter 5.

2 Literature Review

Presented here are the topics deemed to be of relevance to the research work completed in this thesis. The issues affecting Resin Transfer Moulding, in particular processing parameters (Section 2.1.1) and resin characterisation (Section 2.1.2), are discussed in Section 2.1. Fibreglass preform manufacturing is presented in Section 2.2, with the specific case of the Ford Programmable Preforming Process in Section 2.2.1. The Taguchi method of design of experiments is introduced in Section 2.3.1. Section 2.4 includes information regarding surface finish characterisation, with additional attention being paid to the ONDULO surface measurement system in Section 2.4.3. A brief exploration of the concept of preform imaging methods is presented in Section 2.5.

2.1 Resin Transfer Moulding

The increasing demand for less expensive and higher production manufacturing methods has led the automotive industry towards many new techniques and materials. In the past, body components were manufactured by metal stamping, required labour for welding and time for assembly of the many pieces. The introduction of composites in the automotive industry allowed for a number of new manufacturing techniques to be implemented. Among them, RTM has gained a great deal of interest thanks to ability to produce net shape parts, eliminate finishing operations, allow for greater versatility of reinforcement materials, reduced waste rate and higher production times [4].

There are several factors influencing the overall quality of the finished parts produced by RTM, ranging from the processing and mould parameters, to the resin formulation and preform design. Presented in Section 2.1.1 is a review of the issues affecting RTM processing, while Section 2.1.2 examines the influence of resin properties.

2.1.1 Processing Parameters

One of the particularities concerning composite materials is that the processes and tooling required during manufacturing relate directly to the quality of the finished part. In the case of RTM, the outcome of any part moulding is dependent on the quality and temperature of the mould faces, location and pressure of the resin injection and venting.

Previous research aimed to understand the effect each of these parameters has on the moulding process. Karbhari et al. [7] studied the effect of material, process and equipment variables on tension, shear and bending of composite parts using the Taguchi design of experiments method. It was determined that stroke length, an injection piston parameter, had the most influence on the performance of RTM parts. The experiments revealed that depending on the design space studied, some factors appeared to be insensitive to change. Surface finish and filling time were used as response metrics by Dutiro [8] to research the factors affecting RTM processing. Injection pressure, filler content, glass fibre volume fraction and mould temperature were examined using a quadratic design technique. Improved surface finish was seen in cases where injection pressure was increased and fibre

volume fraction decreased, though resin filler content was the most influential factor. Meanwhile, gloss increased with reduced filler content and lower mould temperatures [9]. Bayldon [10] concluded that higher filler content and injection pressure improve roughness and gloss measures, though limiting benefits were observed as the filler caused difficulties in filling the mould cavity.

Work was carried out by Raja [5], seeking to determine optimal process parameters for Class A surface finish in RTM. A surface roughness prediction model was developed to include the effect of LPA content, filler content, temperature gradient between moulds and injection pressure. Test composite panels were manufactured using a fibreglass preform and unsaturated polyester resin system according to an experiment matrix designed based on the Taguchi method. Surface roughness results obtained from a contact profilometer with filter cut-off wavelengths of 2.5 mm, 8 mm and 25 mm were used to establish the value of each fitting constant based on non-linear regression analysis, therefore providing a goodness of fit calculated to be $R^2 = 0.96$. The general form of the model representing the average roughness, R_a (μm), is given by:

$$R_a = e^{(\beta_0+\beta_1 A^2+\beta_2 A+\beta_3 C+\beta_4 E+\beta_5 F+\beta_6 CF)} \qquad \textit{Eq. 2.1}$$

where β_i (i = 0-6) are fitting constants, A is LPA content (wt%), C is filler content (wt%), E is temperature gradient (°C) and F is injection pressure (kPa) [11]. Figure 2.1 displays the 3-D parabola obtained when filler content and temperature gradient are fixed.

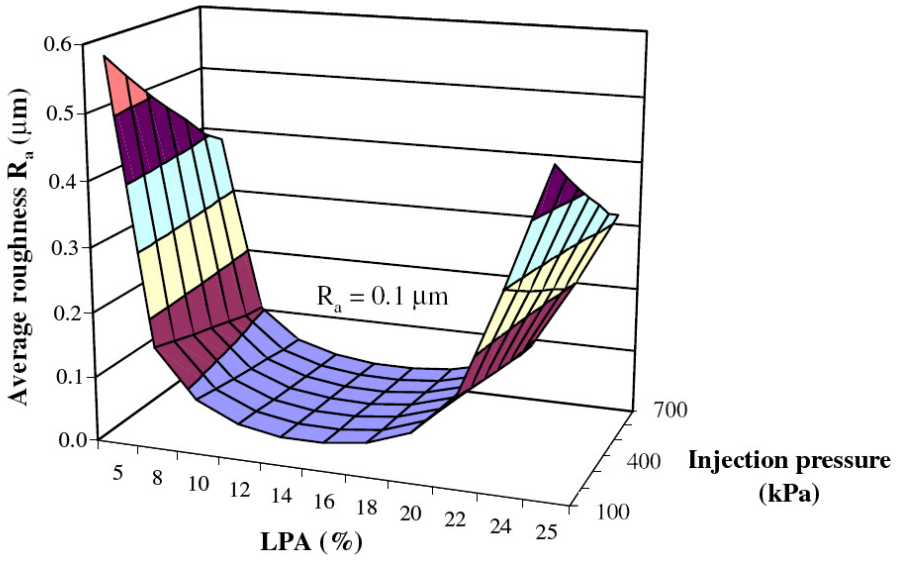

Figure 2.1: Predicted roughness at filler content of 30 wt% and temperature gradient of 15°C for a cutoff wavelength of 2.5 mm [11]

By establishing upper limits of 0.1 µm, 0.2 µm, and 0.5 µm as the acceptable roughness at each cut-off wavelength to obtain Class A surface finish, the design space could further be refined in order to determine optimal parameter values. Based upon cost concerns, LPA content was selected to be 10 wt%, while filler content was set at 30 wt% according to the manufacturer specifications. A 15°C temperature gradient and 621 kPa injection pressure, the maximum possible by the injection pump, were chosen to provide the best surface finish. The selection window for optimum processing, along with the chosen optimum parameters are presented in Figure 2.2.

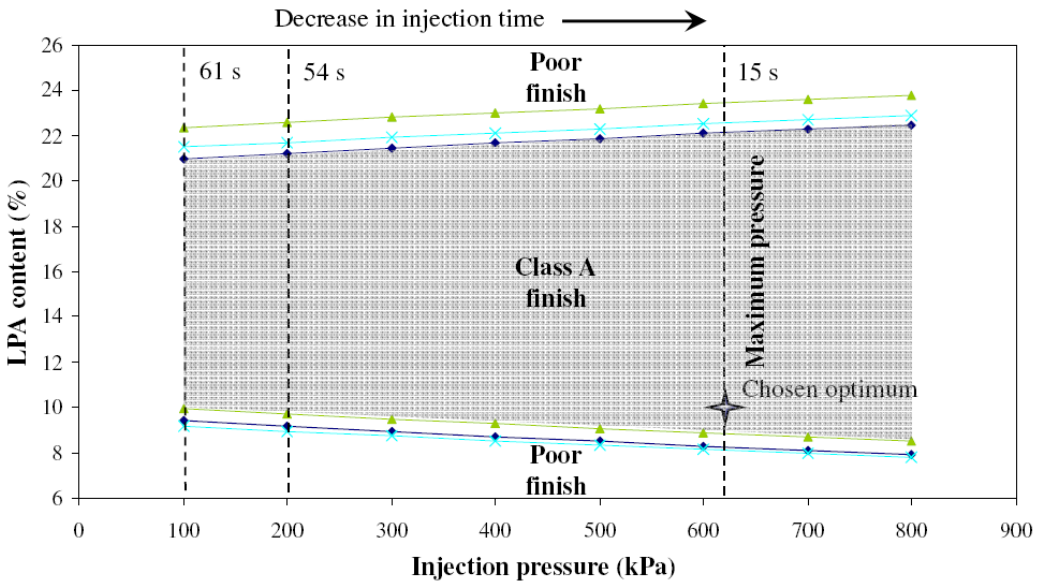

Figure 2.2: Selection window for optimum processing parameters at filler content of 30 wt% and temperature gradient of 15°C, for cutoff wavelengths of 2.5 mm, 8 mm, and 25 mm. The dashed lines indicate the injection time for the preform at the corresponding injection pressure [12].

The results obtained showed significant improvements in surface quality and reduction of injection time to approximately 15 seconds, another attribute of importance to the automotive industry.

2.1.2 Resin Characteristics

The characteristics of the resin system itself are of great importance to the outcome of the RTM process. Polymer resins are increasingly common in the automotive industry thanks to their light weight, corrosion resistance, superior fatigue resistance, energy absorption and noise suppression capabilities [5]. A common issue, however, is the tendency of these resins to undergo volumetric cure shrinkage, resulting in surface defects such as waviness, sink marks and dimensional inaccuracies. Cure shrinkage of 7-10% is typically observed in

unsaturated polyester (UP) resins, thus complicating the task of achieving Class A finish in composite parts [2].

The use of techniques allowing for the thermal, rheological and morphological characterization, have allowed for a better understanding of the resin system. Research on the topic has focused on compensating for the volumetric cure shrinkage by the introduction of thermoplastic particles, called Low Profile Additives (LPA). Although the underlying principles of LPAs are not well understood, much work has been completed seeking to understand their behaviour. Thermal expansion during high temperature cure, phase separation between LPA and UP resin, and micro-void formation at the LPA/UP interface are generally accepted to be the mechanisms behind the expansion of the resin system.

The behaviour of an UP resin system containing LPAs was studied by Raja [13], with the objective of characterising the cure shrinkage. A series of dynamic and isothermal scans using a Differential Scanning Calorimeter (DSC) revealed no significant effect on the total heat of reaction or gel time, though cases with high LPA content (40%) showed slower reaction times. Cure shrinkage was studied by using a specially devised isothermal rheometer test which operated in two segments. First, a constant gap was maintained until the resin reached the liquid-solid transition point, following which the rheometer was set to maintain a constant normal force. Variations in the gap between the plates were used to calculate the change in cure shrinkage. Results of these tests are shown in Figure 2.3.

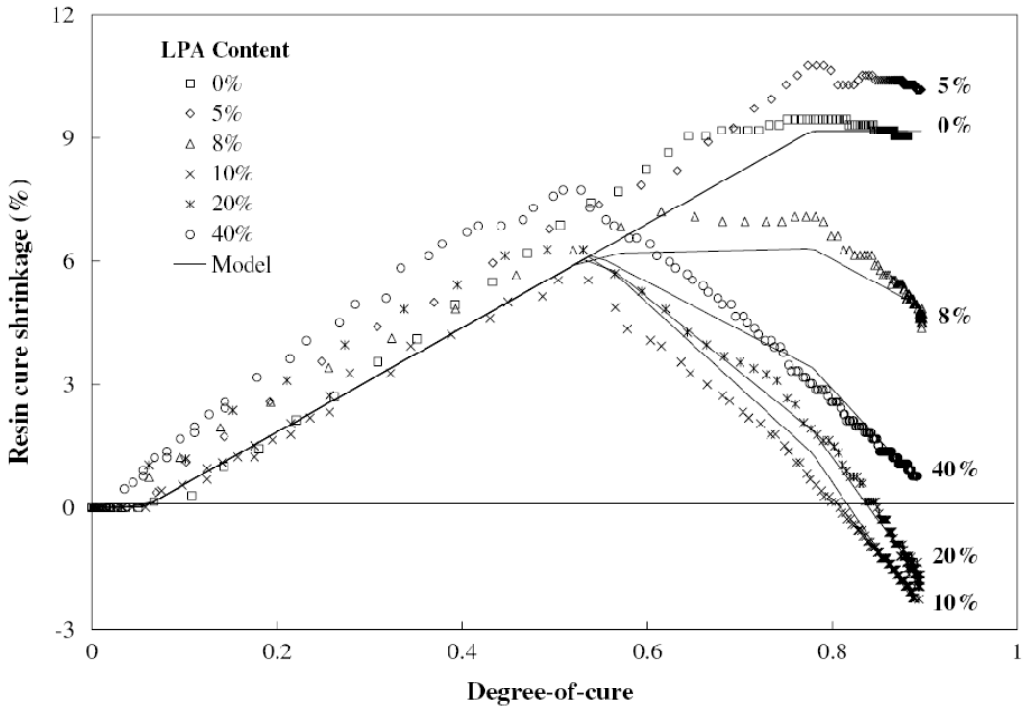

Figure 2.3: Comparison between measured resin cure shrinkage and model prediction under a 90°C isothermal cure condition [13].

Cure shrinkage is compensated for in cases where LPA content ranges from 10-20%, while content of 40% and below 10% still show cure shrinkage in the cured resin. A resin LPA content of 10% was selected as ideal based on phase separation, micro-void formation and minimum cost.

2.2 Fibreglass Preform Manufacturing

Another key factor contributing to the overall quality of composite components is the reinforcement material. In order to replace metal structural, semi-structural and Class A parts, the automotive industry has turned to composites made with reinforcements ranging from carbon and glass, all the way to natural fibres [1]. The great necessity for such applications, however, is the ability to produce high

volumes of strong parts at a high rate and low cost. For Class A components, the standard has been the use of glass fibres, with the Sheet Moulding Compound (SMC) process being most popular [14]. The potential benefits of RTM processing, however, have created a need for high-rate fibreglass preforming, and thus research in the field has grown.

The first step towards the application of high-volume preforming was in 1988 with the creation of the Automotive Composites Consortium (ACC), a research effort fashioned by Ford, General Motors and Chrysler, and sponsored by the U.S. Department of Energy. The program was seeking to carry out pre-competitive research in the area of polymer composites for structural applications. The result was a technique called the Programmable Powdered Preforming Process (P4) which carried out automated deposition of chopped glass fibres. By having screens shaped like the part and with a partial vacuum applied, fibres could be held in place until a powdered binder was sprayed into place and the preform compacted and heated to be consolidated and moved to the resin infusion mould [15].

2.2.1 Ford Programmable Preforming Process

Based upon the expertise gained from the P4 technique, Ford Research and Aston Martin developed the Ford Programmable Preforming Process (F3P) system in cooperation with Sotira Composites. This system, refined by researchers for industrial production, fulfilled the need for fibreglass preforming towards the manufacture of several Aston Martin models, such as the V12 Vanquish

introduced in 2001, which incorporated 26 composite components [3]. Shown in Figure 2.4 are images contrasting the quantity of scrap produced in (a) conventional thermoforming processes, and (b) F3P robotic preforming. Other benefits resulting from the new design technique include the ability to change mould tools quickly (~10 minutes), the flexibility to vary fibre length and areal density accurately, and the capability of manufacturing multiple components for a variety of car models.

(a) Conventional Thermoforming (b) F3P Robotic Preforming

Figure 2.4: Photos contrasting quantity of scrap material obtained during (a) conventional thermoforming, (b) F3P robotic preforming of Aston Martin DB9 RH door opening ring [14]

Developmental work on the F3P system over the past decade have led operators to the selection and use of 3469 tex PREFORMance glass rovings manufactured by PPG Industries Inc., which commingles a thermoplastic polymer 'string' binder directly into the rovings [3]. A fine 1200 tex low-density veil roving supplied by Owens Corning Composite Solutions LLC without any binder is used on surfaces requiring good surface finish. These changes were made to the original system in order to prevent machine clogging that occurred due to the use of powdered binders. Figure 2.5 depicts F3P in its most current form: (a) chopped fibres are

deposited by a spray gun system, (b) heating of stringer binders with forced air consolidates the preform, (c) it is then stabilised by forced cold air before (d), the finished preform is extracted.

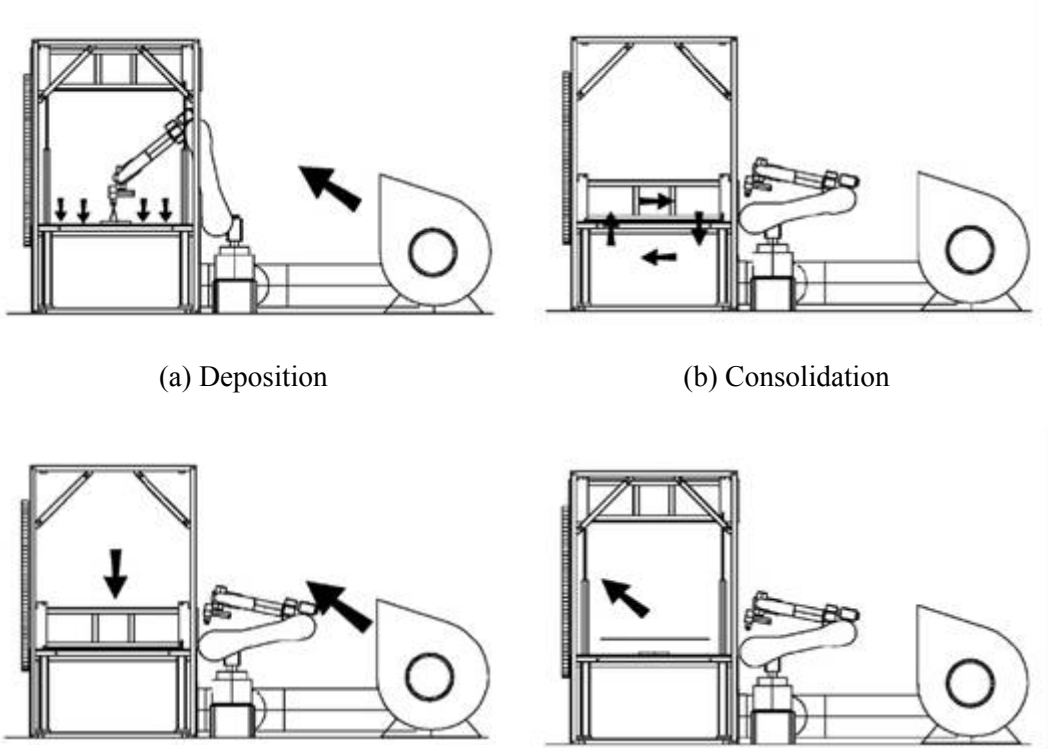

(a) Deposition (b) Consolidation

(c) Stabilisation (d) Extraction

Figure 2.5: Schematic of Ford Programmable Preforming Process (F3P) [16]

Research work was carried out by Dahl et al. [17] seeking to further investigate the influence of fibre volume fraction on processing and performance of RTM composites. Fibreglass preforms manufactured by F3P were prepared with a range of areal densities corresponding to fibre volume fractions of 15-25%, in order to study the effect on permeability and compressibility. Further, sample panels were processed by RTM and submitted to tensile and compressive mechanical testing. Results for the dry preforms showed trends of decreased permeability and

increased compaction pressure as the fibre volume fraction increased. Mechanical testing revealed trends of increasing tensile modulus, strength and strain-to-failure for increased fibre volume fraction – while no influence was seen in compressive strength. Moreover, an observed decrease in permeability existed due to the introduction of surface veils.

Probabilistic and sensitivity analysis was carried out by Bebamzadeh et al. [18], allowing for the calculation of relative importance of a number of processing parameters. Finite element reliability analysis was used to obtain rankings showing distance between fibres, fibre diameter, and volumetric resin cure shrinkage as the most important factors contributing to maximum surface waviness of 0.25 μm.

Based upon input from Aston Martin [19], it is known that the inherent quality of a preform is defined by three factors: fibre selection, machine parameters, and fibre distribution. The selection of the manufacturer and the type of glass fibres and binder systems to be used constitute the fibre selection. Machine parameters include: design of the chopper gun, spray rate, spray pattern, and fibre ejection parameters. As discussed, developmental work has previously been carried out to determine proprietary fibre selection and machine parameters. The variations in fibre distribution are fibre areal density and surface veil thickness. Currently, the sensitivity of Class A surface finish to variations in fibre distribution is not well understood and requires further study.

2.3 Design of Experiments

Experimentation is an important step in the development of any process or the understanding of any concept. Design of Experiments (DOE) is a scientific approach allowing for the study of the relationship between experimental inputs and the resulting outputs. In its most basic of forms, DOE represents the use of statistical analysis to study the effects of multiple factors at once, as opposed to the tedious study of a single experimental parameter at a time. The technique was first introduced by Sir Ronald A. Fisher in England in the early 1920s, with the goal of determining optimum water, rain, sunshine, fertilizer, and soil conditions needed to produce the best crop [20]. Classical DOE consisted of varying factors in order to graph trends in performance and determine the optimal performance for each variable. Much research and development in the field followed, but the applications of classical DOE remained limited to academic environments.

2.3.1 Taguchi Method

Enter Dr. Genichi Taguchi, who developed a new technique with the idea in mind that quality is measured by consistency of performance. Referred to as the Taguchi method, this technique seeks to reduce the distance between the mean and the target value, as well as minimise the standard deviation in the results obtained for a given test population [21]. This is accomplished thanks to the use of a set of tables, known as orthogonal arrays, which enable the main variables in a given experiment to be investigated in a minimal number of trials.

The Taguchi method is prepared for a given application in several steps. First, the objectives of the project are determined, with specific quality characteristics and evaluation metrics established. This is carried out by researchers with knowledge of the given design space and experiment scope. Next, a broad set of factors thought to influence the results are considered, and the number of trials to be completed is selected. The suspected behaviour of each variable, along with the number of degrees-of-freedom which the orthogonal array can accommodate, is used to establish the number of levels to be studied. Finally, the key factors which suit the experiment plan are chosen based upon the size of the design array. The result of this preparation is a test matrix consisting of the most significant factors studied at specific variable levels.

The next step in the Taguchi method is the carrying out of the experimental trials as planned, thus generating results based on the evaluation of the samples which allow for statistical calculations to be completed. The formulas and procedures used for the Taguchi method are referred to as Analysis of Variance (ANOVA). It accounts for variability over multiple trials by calculating how much the variation in each factor contributes to the total variations observed in the results. Further, within this analysis, the consistency of performance is measured by what is called the Mean-Squared Deviation (MSD), which allows for the study of all sorts of data. Depending on the desired criteria, either the minimum MSD or trends within each factor can be used to determine optimal parameters for a given experiment, as well as the corresponding estimated performance.

2.4 Surface Finish Characterisation

The surface of an object can be defined as the boundary that separates it from the surrounding medium, as per the ANSI/ASME standard [22]. This is a very broad description of the concept, but it provides a good basis for characterisation to be carried out. One can imagine that if a material was cut and the cross-section were analysed, it would be the 2-D profile produced by the boundary of this object that would be of interest. The profile of this boundary is referred to as the surface texture, and can be decomposed into a number of superimposed profiles of varying wavelength [23], as depicted in Figure 2.6 [24].

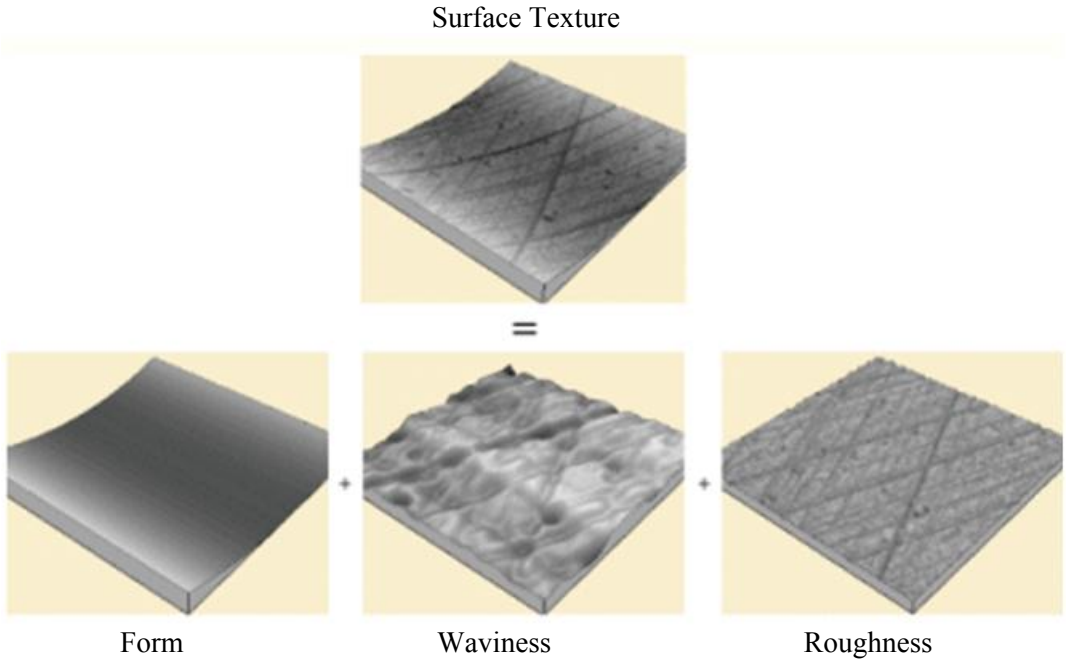

Figure 2.6: Decomposition of surface texture into form, waviness and roughness [24]

Roughness is the category representing the profiles made up of the shortest wavelength, and is commonly seen as originating from the irregularities that are inherent to the given production process. Waviness is the next order of lower

frequency and comes from a variety of causes. Finally, form is the longest wavelengths, and represents the deviations from the nominal surface shape.

2.4.1 Class A Surface Finish

'Class A' is a term used to describe the finish deemed to be acceptable for exterior parts in the automotive industry. Dutiro describes Class A finish as exhibiting "aspects of flatness, smoothness, and light reflection similar to that of finished stamped steel sheeting, typically with a DOI (Distinctness-of-image) values between 60-90, as measured with D-Sight optical enhancement techniques" [9]. There is no one standard, but components should be aesthetically pleasing, smooth and without noticeable defects – thus mimicking an equivalent metal component which is perfectly polished, free of porosity or scratches, and with a high lustre finish. In industry, composite components are polished, primed, and then finished with paint which is sprayed over allowing for inconsistencies to be filled. The cost and labour required for this work, however, can be reduced by improving processing methods and moulding techniques. The use of resin formulations that appropriately compensate for expansion/shrinkage mechanisms, as well as appropriate tool and processing parameter design allows for superior part quality.

2.4.2 Surface Texture Measurements

The techniques used in order to map the profile of a given surface can be categorized as contact or non-contact methods. Contact methods scan the

topography of a given surface based upon the displacement feedback from a stylus dragged across a given surface, as depicted in Figure 2.7. The surface must be rigid and the resolution of the readings depends on the diameter of the stylus tip used. Non-contact methods make use of optical techniques based on the concepts of light reflection and thus require high-gloss parts for the best readings. Several systems have been developed specifically for the automotive industry, such as the Quality Measurement System, the BYK wave-scan, the D-Sight, and the ONDULO system [25].

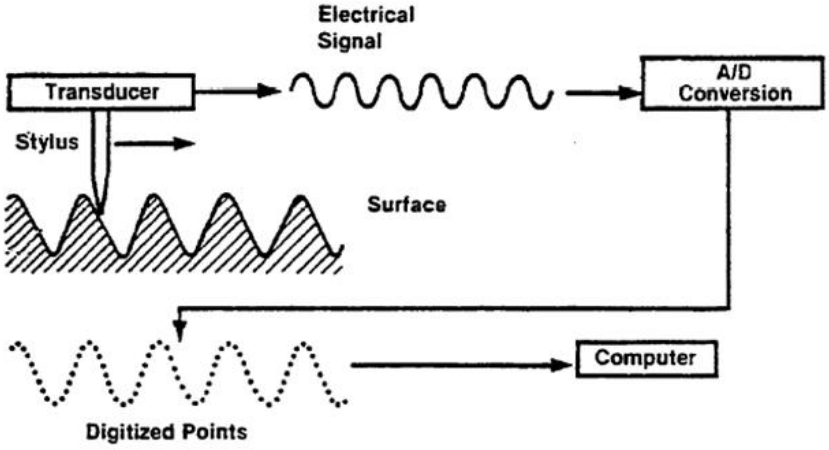

Figure 2.7: Schematic diagram of contact stylus instrument [26]

2.4.3 ONDULO Measurement System

A technique of interest is the ONDULO measurement system, designed specifically for the automotive industry to observe surface defects present on Class A parts [6]. Developed by Visuol Technologies (Saint-Julien-lès-Metz, France), it operates based on the principle of deflectometry, evaluating at high resolution the radii of curvature of defects on a given surface [27]. The device

setup is diagrammed in Figure 2.8, showing an UXGA camera capturing the reflected image of a geometrical pattern projected onto a screen in a darkened room. Captured images are processed by the software accompanying the ONDULO device in order to extract relevant surface roughness data.

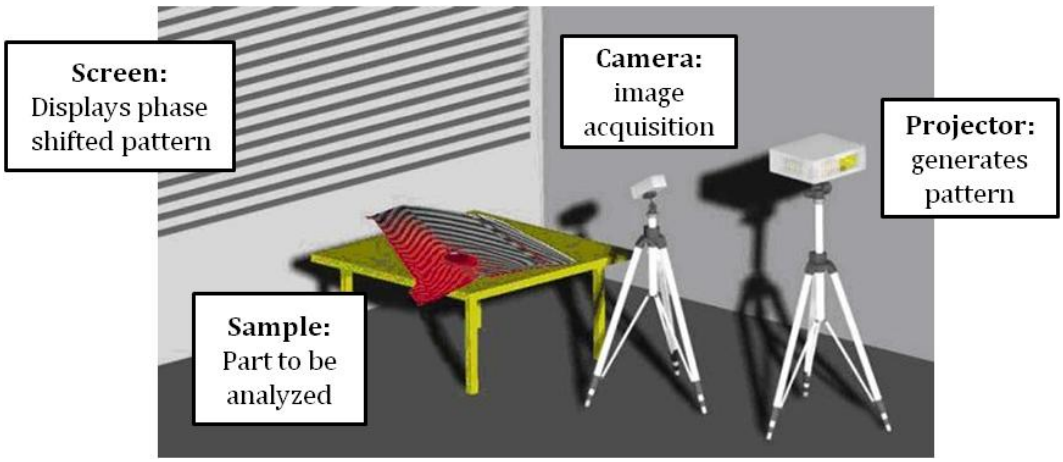

Figure 2.8: Diagram of ONDULO measurement system [27]

2.4.4 Roughness Calculations

For Class A samples, it is common to study the roughness component of the surface texture in order to quantify the part finish. A cut-off wavelength must be selected with the purpose of observing profiles representing only the shortest wavelength irregularities. The standard calculation carried out on the data in the desired range is referred to as the average roughness, R_a, which is defined as the arithmetical mean of the absolute values of the profile deviates (Y_i) from the mean line:

$$R_a = \frac{1}{n}\sum_{i}^{n}\left|Y_i\right| \qquad \textit{Eq. 2.2}$$

Work carried out by DeBolt [28] studied the effectiveness of several measurement techniques and roughness calculation wavelength cut-offs. Band pass filtering was carried out on the profiles obtained, after which the surface finish was quantified within certain frequency ranges. It was determined that selection of appropriate cut-off wavelengths was of critical importance to understanding the quality of a Class A surface. Palardy [12] utilised both a contact profilometer, and the contactless ONDULO system to study the effect of painting processes on the surface finish of RTM panels. For the evaluation of R_a, a cut-off wavelength of 2.5 mm was used, as per ISO 4288:1996 [29]. This allowed for differences in finish quality to be measured and compared, thus permitting the establishment of optimal process parameters. Schubel et al. [30] studied the surface quality of coated and uncoated composite panels. It was determined that the mean roughness parameter is suitable for relating bare laminates to final painted quality, and that light reflectometry correlates well with subjective assessments for painted laminates.

2.5 Preform Imaging Methods

Little work has been carried out in the literature studying the use of digital imaging to qualify fibreglass preforms prior to RTM manufacturing. This is a technique conceived so as to obtain relevant information regarding attributes such as variations in local areal density, top surface patterns, and presence of defects. The gathered information can be used to validate the adequacy of a preform, or predict the finished outcome following resin injection moulding. The work carried

out in this project on the topic of preform imaging is a novel adaptation of this concept.

Recently, a study that parallels the work in this project has been carried out by Gan et al. [31] at the University of Auckland. This work, as yet unpublished, studies the variability of reinforcement material using a 'lightbox' upon which samples could be placed and photographed by a mounted digital camera. By calculating the discrepancy between a platform with and without a preform present, a gray level value representing the light blocked by the preform is calculated. Analysis of pixel values allows for the determination of localised areal density calculations, and thereafter the ability to proceed with statistical preform characterisation.

2.6 Summary of Literature Review

The purpose of this chapter has been to present the literature reviewed during the course of the research carried out for this project. A great deal of information was gathered concerning the optimization of processing Class A composites by RTM. The most influential factors contributing to good surface finish are injection pressure, control of volumetric cure shrinkage/expansion, mould surface quality, and resin filler content. Further, an understanding of the use of Low Profile Additives (LPA) to compensate for volumetric changes was gained.

An investigation into the Ford Programmable Preforming Process (F3P) revealed the importance of machine, material and architecture parameters. Much

developmental work has already been completed in industry, though further study is required regarding the effect of fibre distribution on surface finish.

The Taguchi method of design of experiments is preferred for design of experiments, having successfully led previous researchers to the determination of optimal experiment parameters, in addition to understanding of the process studied.

Characterisation of surface finish has previously been accomplished by through the use of average roughness (R_a) values, calculated from line profiles extracted from surface topography. This data has successfully been obtained from both contact (stylus) and non-contact (optical) methods. The ONDULO system, a non-contact method, is a technique of interest, thanks to its design specifically for the purpose of imaging Class A surfaces in the automotive industry.

2.7 Research Objectives

The current work is one of the final pieces of the puzzle in a collaborative effort with research groups from the École Polytechnique de Montréal and the University of British Columbia. As part of the Auto21 Network of Centres of Excellence, this project, entitled "Optimization of Composite Manufacturing by Resin Injection", aims to help fulfill the promise of RTM manufacturing in the automotive industry. The role of McGill University in this project is to characterise the resin and preform materials through the use of RTM experiments, focusing mainly on the sensitivity of Class A surface finish to these parameters.

This thesis builds upon the resin characterisation and process optimization carried out by Mohsan H. Raja's PhD thesis [5] and Geneviève Palardy's Master's thesis [2]. Their research investigated the manufacture of composite parts by RTM according to six parameters: LPA (wt%), styrene (wt%), filler (wt%), gel time (min), temperature gradient between moulds (°C) and injection pressure (kPa). A total of 18 fibreglass/UP test panels were moulded and evaluated as per the Taguchi method. A contact profilometer was used to quantify surface roughness, and results were studied by ANOVA, following which a set of optimal parameters were established. Validation test samples were manufactured, and resin volumetric changes were studied using cure kinetics and rheometry methods. Further, the sensitivity of the surface finish to typical painting processes was studied, and ideal heating cycles were suggested.

The objective of the current work is to study the effect of preform variability on the surface finish of Class A composite parts manufactured by RTM. The main goals to be accomplished are:

1. Determine preform characteristics: Preform attributes of interest to surface finish will be selected and a test matrix suitable for investigating variability will be established.
2. Determine quality of dry preforms: A method by which preforms can be qualified prior to injection moulding will be established.
3. Surface finish characterisation: Test composite panels will be manufactured, after which surface roughness will be evaluated.

4. Relate results to surface finish: The variations in preform quality prior to and following moulding will be related.

3 Experimental Procedures

Presented is an outline of the experimental procedures used to study how the variability of fibreglass preforms effects surface finish in Class A composite parts. Section 3.1 describes the materials used throughout the experimental portion of this project. Section 3.2 contains the details regarding the formation of an appropriate experimental test matrix. Next, a novel preform imaging technique used in this thesis is explained in Section 3.3. The RTM process employed for the manufacture of composite test panels is detailed in Section 3.4. Finally, the procedure applied to obtain measurements characterising the surface finish of test panels is detailed in Section 3.5.

3.1 Materials

The set of materials used for experimentation consisted of fibreglass preforms produced by the F3P technique, and an unsaturated polyester (UP) resin obtained from Scott Bader Company Ltd.

3.1.1 Fibreglass Preforms

Preforms were obtained from Sotira Composites according to specifications as determined by the orthogonal array established via Taguchi design of experiments (Section 3.2). Individual samples were cut to 26 cm x 24cm from the 80 cm x 120 cm sheets received. The architecture of the preforms consisted of structural fibres symmetrically sandwiched between layers of surface veil fibres, as seen in Figure

3.1. On the side meant to be for Class A finish, the veil fibres were sprayed down in a criss-crossing manner, thus creating a lattice pattern.

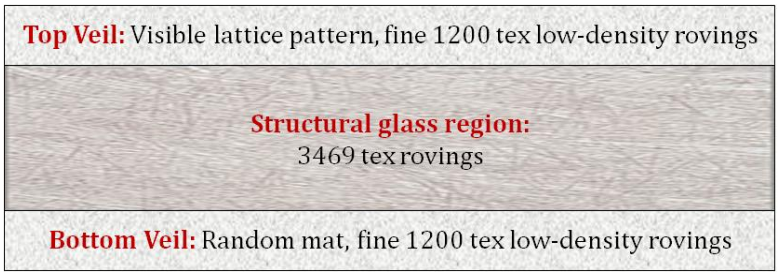

Figure 3.1: Diagram of cross-section of dry F3P fibreglass preform

Developmental work on the F3P system over the past decade has led operators to the selection and use of 3469 tex PREFORMance glass rovings, which commingles a thermoplastic polymer 'string' binder directly into the roving. A fine 1200 tex low-density veil roving without any binder was used on surfaces requiring good surface finish. Details regarding the glass fibres used in the F3P method are listed below:

- Structural Fibres: PPG Industries Inc. – PREFORMance
    - 3469 tex rovings
    - 25.4 mm fibre length
    - Contains up to 6-7 wt% string binder
- Veil Fibres: Owens Corning Composite Solutions LLC
    - 1200 tex low-density veil rovings
    - No binder present

3.1.2 Unsaturated Polyester Resin

The composite matrix system used for processing consisted of Scott Bader PD9551 unsaturated polyester resin with 10 wt% LPA pre-mixed. The LPA used was PD9419, a polymer solution containing polyvinyl acetate (PVAc) and polymethyl methacrylate (PMMA). The initial resin mixture was combined with 30 wt% OMYA BLR®2 calcium carbonate filler, 0.5 wt% AkzoNobel cobalt 2-ethylhexonoate accelerator, and 2.6 wt% AkzoNobel Trigonox®93 (tert-butyl peroxybenzoate) catalyst. The details regarding the resin constituents, as well as specific properties of the neat UP resin are presented in Table 3.1 and Table 3.2 respectively. The procedure used to prepare the resin prior to injection is outlined in Section 3.4.1.

Table 3.1: List of resin constituents

Type	Name	Company	Weight%
Resin	PD9551	Scott Bader Ltd	---
LPA	PD9419	Scott Bader Ltd	10%
Filler	$CaCO_3$ BLR®2	OMYA	30%
Accelerator	1% Cobalt solution, Cobalt 2-ethylhexonoate	AkzoNobel Chemicals	0.5%
Catalyst	Trigonox®93, tert-butyl peroxybenzoate	AkzoNobel Chemicals	2.6%

Table 3.2: Specific properties of the neat unsaturated polyester resin [5]

Thermal Conductivity (W/mK)	Reaction Enthalpy (kJ/kg)	Specific Heat (J/kgK)	Density (kg/m^3)
0.25	400	1600	1260

3.2 Design of Experiments

The first step towards understanding the contribution of F3P fibreglass preforms to the surface finish of Class A parts is characterising the preforms themselves. Thus, the factors which are known to contribute to the quality of a preform must be understood such that variability may be studied. Based upon input from Aston Martin, it was concluded that the inherent quality of a preform was defined by three factors: fibre selection, machine parameters, and fibre distribution. As previously discussed, much developmental work has been carried out in order to select the appropriate materials for F3P. Additionally, although the actual machine parameters would be of interest to study, an intimate knowledge and direct access to the system would be required – this was not possible due to the fact that the F3P setup is already involved in manufacturing on the order of 50 000 units per year.

3.2.1 Taguchi Method

Thus, it was decided that the focus of the project would be to study how fibre distribution affects surface finish. For the purposes of this research, the Taguchi technique for design of experiments was implemented. Planning a set of experiments according to this technique required first the selection of primary objectives and metrics by which results could be measured and compared. For this project, the goal was to study the contribution of fibre reinforcement parameters using mean roughness values calculated from measured surface profiles. Next, starting from a wide range of contributors, the most important factors were

selected. Having dismissed fibre selection and machine parameters, the focus was set on fibre distribution – within which the two major factors easily varied and of importance to surface finish are the preform areal density and the weight fraction of the surface veil. Taking into consideration the known acceptable range and the potential number of trials required, it was decided that the factors would be studied on 4- and 2-levels respectively.

Previously, for work carried out by Raja [5], the F3P system was programmed to output a glass fibre areal density of 1626 g/m^2, which corresponds to a fibre volume fraction (V_f) of 20% for parts with a thickness of 3.175 mm. The structural fibres totalled 81.8% of the total weight fraction of the preforms, with each of the top and bottom veil fibres equalling 9.1% by weight of the preform.

As the final step towards the formulation of a test matrix, the specific levels of each factor were selected. Assuming that surface finish could be improved by increasing the resin content and thickening the surface veil, factor levels exploring the range of surrounding the 20% volume fraction and 9.1% veil weight fraction were decided upon. Having determined that the experiment would consist of one 4-level and one 2-level factor, the Taguchi technique dictated that the minimum number of trials needed would be 8, thus making use of an upgraded L-8 array, as presented in Table 3.3. It is important to note that values of fibre volume fraction are calculated based on the moulded part thickness of 3.175 mm, thus values of 14%, 17%, 20%, and 23% corresponded to fibre areal densities of 1138, 1382, 1626, and 1870 g/m^2 for dry preforms. Also, the top veil wt% and bottom veil

wt% will always be identical since the F3P preforms obtained were designed to be symmetric apart from the existence of the top veil lattice pattern.

Table 3.3: Experiment matrix developed by Taguchi method

Set	Preform V_f (%)	Top Veil wt%
1	14	10
2	14	15
3	17	10
4	17	15
5	20	10
6	20	15
7	23	10
8	23	15

3.3 Preform Imaging Technique

Since local variations in the quality of fibreglass reinforcements are not obvious following injection moulding, it is of interest to obtain images detailing the fibre distribution of preforms in their dry state prior to moulding. The hope of this exercise is to gain further information regarding the relative quality of preforms and how it relates to moulded parts. A novel technique whereby fibrous reinforcements were photographed with the goal of emphasizing local changes in areal density was implemented in this project.

3.3.1 Light Transmission Fixture

The test setup consisted of a fluorescent light source enclosed in a box and capped by a 3.175 mm white acrylic sheet serving as a light diffuser. Dry fibrous reinforcements were placed onto the acrylic sheet and photographed such that a

totally whitened background appeared. Images were photographed using a SONY Alpha digital SLR camera, model A200, at a resolution of 1920 x 1280 pixels at 72 dpi, placed 102 cm from the sample. It was critical that all camera settings were kept constant throughout, thus the exposure was set to 1/50, the aperture to F5, ISO 100 and focal length of 60 mm. The setup was placed in a darkened room, where samples could be photographed without interference from ambient lighting. Figure 3.2 illustrates the setup used to obtain light transmission images of dry preforms, as well as a sample image obtained from the imaging setup.

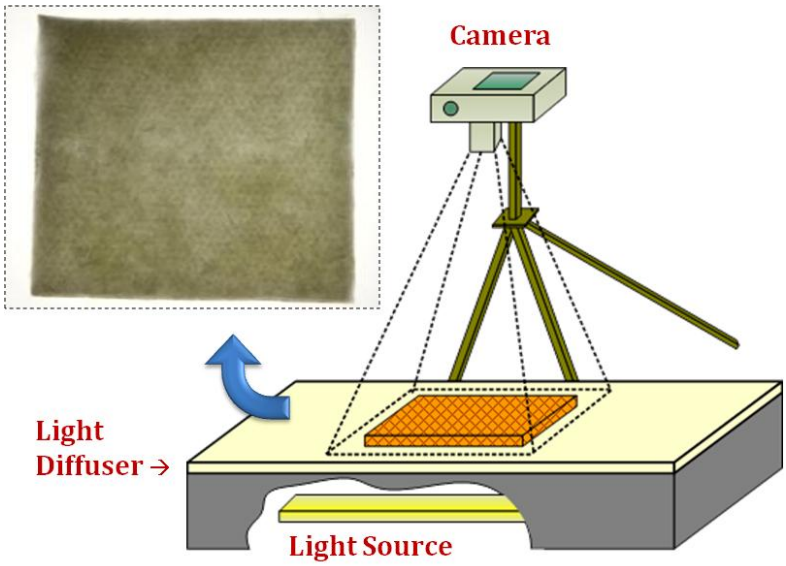

Figure 3.2: Diagram of fixture used to image light transmission through dry preforms, with sample of acquired image shown in upper-left corner

3.3.2 Image Analysis

The digital images obtained from this technique were then analysed using custom code created for MATLAB computing software, as described in Figure 3.3.

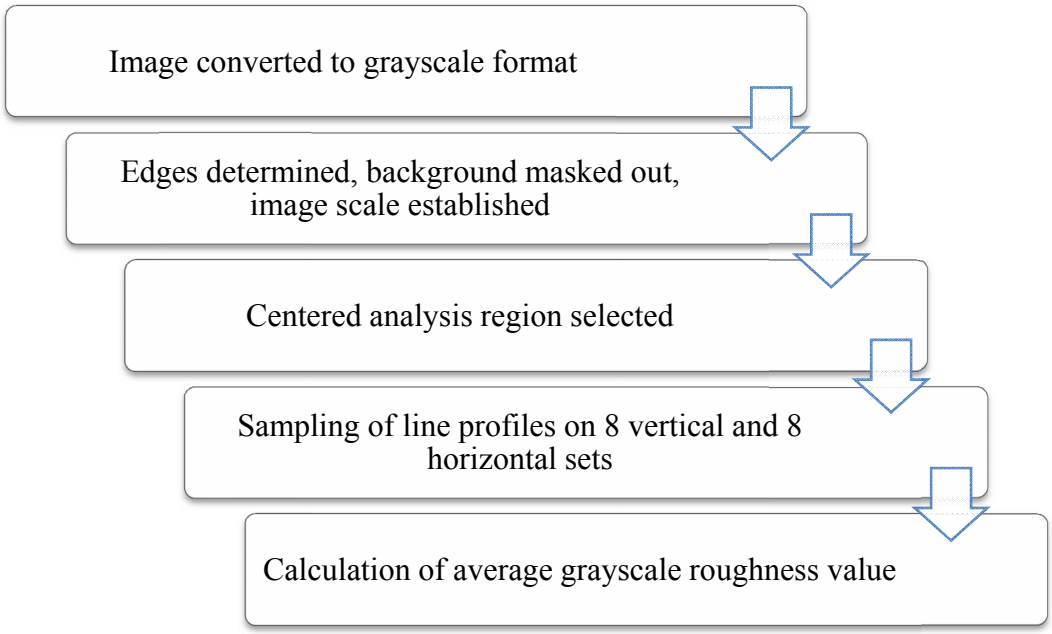

Figure 3.3: Diagram of main steps involved in image analysis using MATLAB code

Each image was converted to grayscale format, following which the outer edges of the preform were determined and used to mask out the background pixels. The boundary of the preform was then used to approximate an image scale and establish a centered region within which line profiles of the grayscale values could be extracted. This technique of sampling 8 sets of vertical and horizontal line profiles was meant to mimic the process used by Palardy [2] to measure the surface quality of moulded parts. In order to quantify the surface of the preforms based on the images obtained, a pseudo-roughness value was established. In a manner paralleling the calculation of average roughness values (Eq. 2.2), R_a. the deviation from the mean (Y_i) of each line profile was used to obtain a value henceforth referred to as the average grayscale roughness value, G_a, seen in Eq. 3.1.

$$G_a = \frac{1}{n}\sum_{i}^{n}\left|Y_i\right| \qquad \textit{Eq. 3.1}$$

The values obtained were measured in units of grayscale intensity, and provide a basis for comparing dry preforms to each other. Better overall surface quality should exist in those preforms that demonstrate the lowest grayscale roughness values, since the deviation from the mean should be smallest in cases where the preform has more uniform light transmission. The complete custom MATLAB image analysis code can be found in Appendix A.

3.4 Resin Transfer Moulding

The RTM processing and resin characteristics utilised in this section are those developed by previous researchers and deemed to be optimal for the current experimental setup [5].

3.4.1 Moulding Process

The manufacture of composite test panels was completed using an industrial hydraulic press fitted with a flat steel mould incorporating a circulating water heating system. Fibreglass preforms were placed within a 3.175 mm thick picture frame with a 26 cm x 24 cm opening, as shown in Figure 3.4.

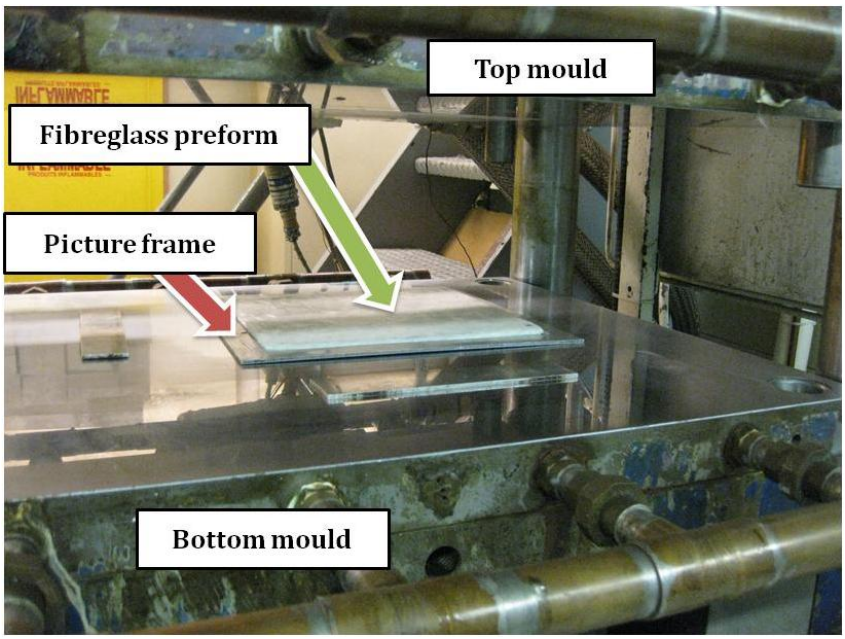

Figure 3.4: RTM setup showing the press platens with the preform in the picture frame

The steps required for manufacturing were followed in a systematic manner, so as to retain identical parameters throughout. Prior to moulding, the mirror-like finish of the mould was carefully cleaned and treated with Chem-Trend Chemlease PMR-90, a release agent specially designed for Class A finish. Chemlease 70-90 release agent was applied to the picture frame, metal shim spacers, as well as the components of the injection pump that would come in contact with the resin. For both release agents, two layers were applied then buffed away with a 10 minute gap between application, and a 30 minute wait following the final coat. A Conair circulating water heating system was used pre-heat the top and bottom moulds to 75°C and 90°C respectively. The preform was positioned within the picture frame mould, then onto the mould surface such that the Class A side containing the lattice pattern was facing down. Also, since the inlet and vent ports were designed to create a uniform linear flow front through the fibreglass preform, a 6.35 mm

separation was created between the edge of the picture frame and the preform on the inlet side. Adhesive-backed GORE-TEX® expanded-PTFE was applied to the setup to ensure proper sealing of the interface between the mould and the picture frame.

The resin system described in Section 3.1.2 was prepared in batches of 500 g by first adding 30 wt% filler to the pre-mixed resin/LPA, then 0.5 wt% accelerator and 2.6 wt% catalyst in successive steps. A dual-propeller mixing attachment mounted on a drill press was employed to thoroughly mix the resin following each step. Once prepared, the resin was poured into the barrel of a Radius Engineering pneumatic-controlled injection pump remaining at room temperature. With the moulds heated to the desired temperature, pressure was applied on the picture frame and the resin was injected at a constant pressure of 621 kPa. The exit port was left opened until the point when the entire preform was infiltrated and excess resin began to leave the cavity, at which point the exit flow was blocked. The process was stopped after approximately 30 minutes, corresponding to when the resin was cured, as indicated by the plateau achieved at the maximum pressure level. The finished part was removed and left to cool outside the mould setup.

3.4.2 Data Acquisition System

The setup was instrumented with Dynisco PT422 pressure sensors and type J thermocouples connected to a Vishay System 6000 data acquisition system (DAQ) allowing for the cure development to be monitored. Four pressure and four temperature sensors were embedded in the top and bottom mould, while five other

temperature sensors were attached at various locations externally. An additional pressure transducer was employed to observe the pressure maintained in the injection pump. The live development of the pressure curves was monitored to know when curing was complete, in addition to data being acquired at 10 samples per second throughout the entire RTM processing.

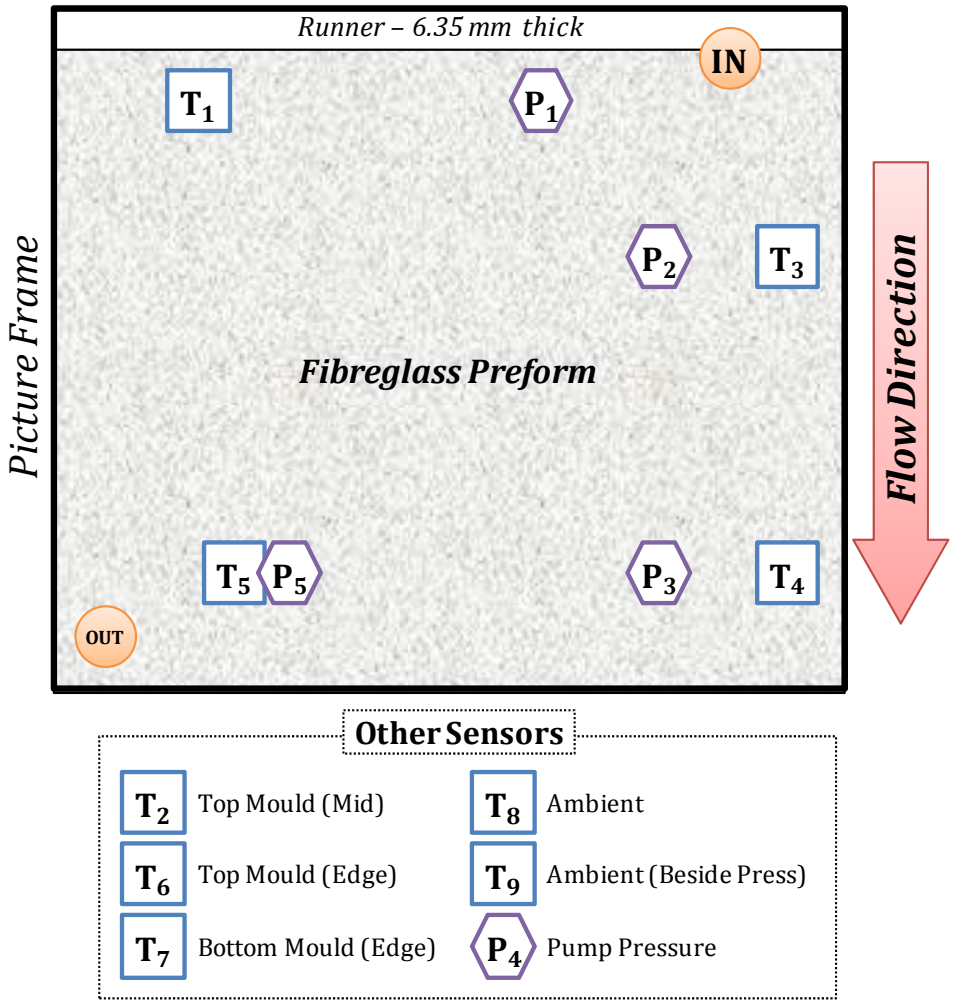

Figure 3.5: Position of temperature (T_i) and pressure (P_i) sensors connected to DAQ and mounted on RTM press

3.4.3 Mould Surface Finish

In order to verify the quality of the finish on the bottom mould, surface roughness measurements were carried out using a Mitutoyo Surftest 401 Portable Tester. Sets of profile scans were run at the four corners and centre of the area of interest. The profilometer's diamond stylus of radius 5 μm had a driving speed of 0.5 mm/s and a sampling rate of 400 points/s, allowing for values as small as 0.01 μm to be read. The average roughness, R_a, measured with a cut-off wavelength of 2.5 mm had a mean value of 0.5 μm, with values ranging from 0.4 μm to 0.6 μm.

3.5 Surface Finish Measurement

For this research, each composite panel was first imaged using the ONDULO system, following which a representative sample sized 80 mm x 80 mm was identified for surface quality measurements.

3.5.1 ONDULO Measurements

The Visuol Technologies ONDULO system was utilised for the purpose of imaging and qualifying the surface finish of manufactured composite panels. The samples were placed upon a table positioned between a digital camera and a projection screen in a darkened room, as seen in Figure 3.6.

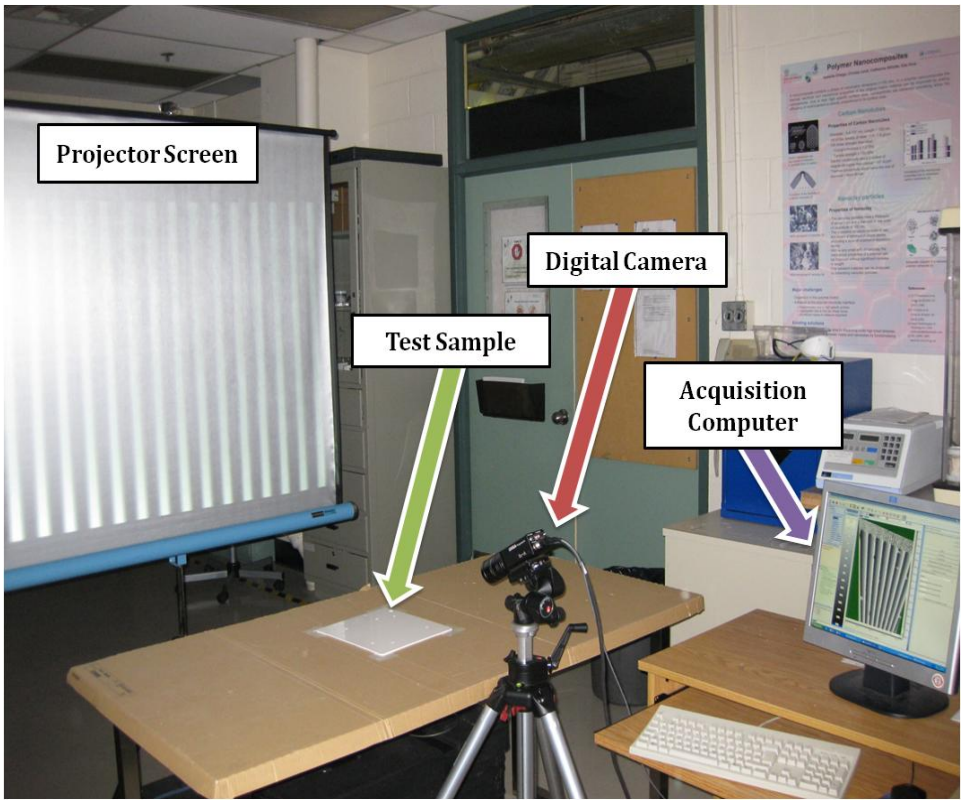

Figure 3.6: Photograph of ONDULO setup, with composite panel placed between digital camera and projector screen with phased pattern

A progressive scan SONY XCLU1000 black and white UXGA digital video camera was used to capture high-resolution images of the various geometrical patterns projected onto the screen during the acquisition cycle. Once rectified by the acquisition software, these images displayed the test panels in their entirety, though the conical line of sight of the 16-mm lens produced a trapezoidal region outside of which no data was present. Calibration of the ONDULO system was carried in two steps: first a specific grid pattern was used to align vertical and horizontal orientations, and then a mirror was employed to establish the optimal reflection conditions. Details regarding the specific calibration and acquisition constants are presented in Table 3.4.

Table 3.4: List of ONDULO parameters established during testing

Parameter	Value
Camera lens	16 mm
Vertical/horizontal size of pixel	4.4 μm
Integration time	350 000
Number of phased lines	16
Width of projection screen	1210 mm
Distance from screen to sample	1570 mm
Distance from sample to camera	420 mm
Angle from camera to sample bed	60°

3.5.2 Roughness Calculation

The images acquired by the ONDULO system were passed over to DigitalSurf MountainsMap Topography XT software in order to extract roughness measurements. Readings from the Y-direction amplitude capture were used to select representative regions for each test sample. These were areas measuring 80 mm x 80 mm which were deemed 'best' on the given test panel. All obvious defects or manufacturing errors were excluded from the measured areas.

The representative region for each sample was filtered using a cubic spline method (ISO/TS 16610-22) with a cut-off wavelength of 8 mm. In a manner similar to the procedure used for dry preform imaging, 8 vertical and 8 horizontal evenly spaced line profiles were extracted. Based upon ISO 12085, a standard used in the automotive industry aiming at studying the functional aspects of a profile, roughness motif calculations were carried out on each line profile. The average roughness value obtained was the mean value of all the individual vertical and horizontal values measured.

3.6 Summary of Experimental Work

Fibreglass preforms manufactured according to the F3P method were obtained in sheets sized 120 cm x 80 cm from Sotira Composites for testing. Using a 26 cm x 24 cm standard cutting template, three samples were prepared for each test set. One session was needed to complete the imaging of all dry cut preforms for light transmission. Next, the two preforms from each set deemed best by observation were individually manufactured by RTM into test panels, with the processing procedures remaining unchanged throughout and being carried out in a randomly selected order. Finally, analysis was carried out to determine relative surface finish quality, first by observation, then utilising the ONDULO system.

4 Results and Discussion

A description of the results and observations concerning the 16 test panels manufactured follows. For reference, the samples will be labelled using "Set-Test" as the format, therefore test 3-2 would refer to the second test sample from Set 3. The outcome of work employing a novel preform imaging technique will be discussed in Section 4.1. Details regarding RTM processing will be presented in Section 4.2, before surface finish measurements are disclosed in Section 4.3. Section 4.4 includes the analysis of variance for the results obtained, while Section 4.5 discusses the relationship between the various outcomes.

4.1 Preform Imaging Technique

Photographs taken using the novel imaging fixture are described in Section 4.1.1, following which the procedure used to obtain relevant data is discussed in Section 4.1.2.

4.1.1 Light Transmission Imaging

The light transmission imaging setup used for this work was designed to obtain information regarding the overall quality of dry preforms prior to moulding. A preform from Set 2 (V_f = 14%, Top Veil wt% = 15%) is shown imaged with the Class A side facing up in Figure 4.1, and then facing down in Figure 4.2. It is clear that the images obtained are not identical when photographed from either side, but rather demonstrate a combination of darkness in areas where light is

blocked, and detail picked up from the fibres on the top of the given side. The system was therefore configured such that the top-most fibres would be in focus, thus emphasizing the lattice that exists in the surface veil. Evidence of greater areal density corresponding to darker regions on the image is provided by observing the top-left most corner in Figure 4.1, and the bottom-left corner of Figure 4.2. These correspond to the same portion of the preform viewed from the top and bottom perspective. The fact that the region is darker is a result of bunching of fibres during preform cutting creating a more fibrous region.

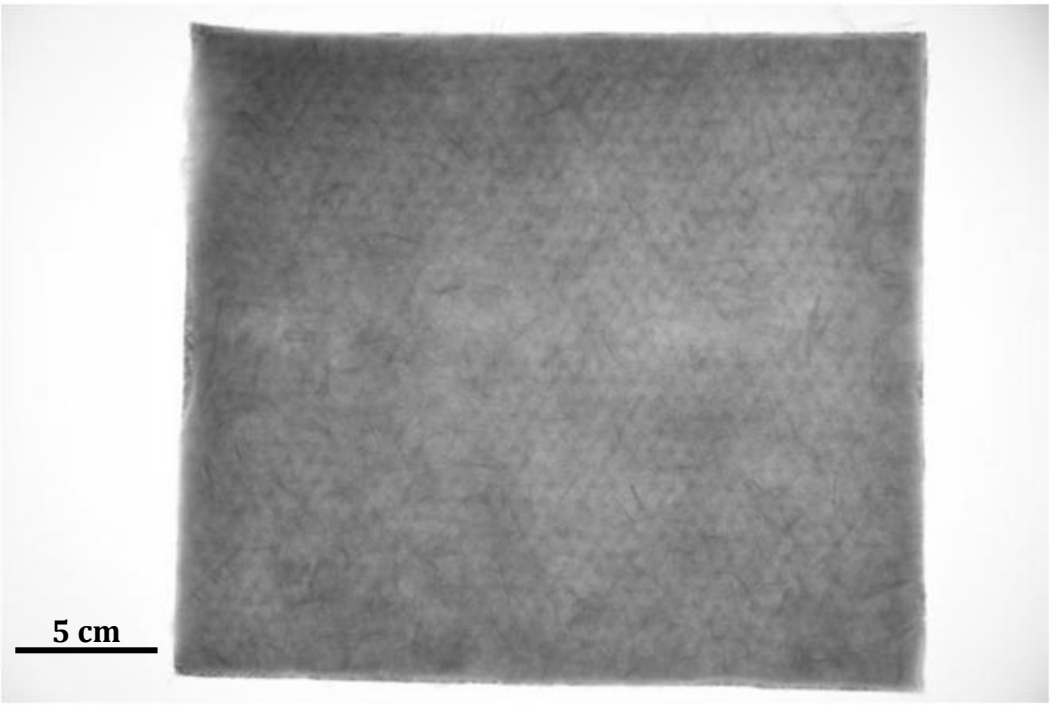

Figure 4.1: Image of preform from Set 2 (V_f = 14%, Top Veil wt% = 15%) with Class A side facing upwards

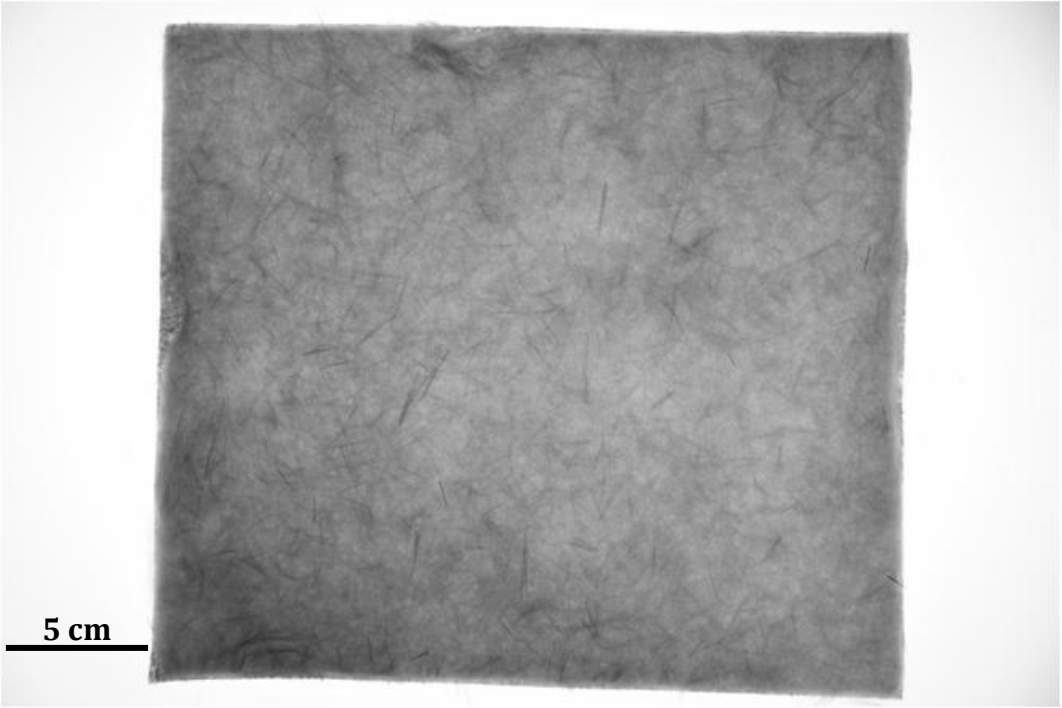

Figure 4.2: Image of preform from Set 2 (V_f = 14%, Top Veil wt% = 15%) with Class A side facing downwards

There was a faint, but noticeable difference in the overall darkness of the images, however, the image analysis calculations are not affected since the mean grayscale roughness value, G_a, represents an averaged deviation from the mean grayscale pixel intensity.

4.1.2 Image Analysis

Each of the images acquired by the light transmission imaging was then processed by custom code created for MATLAB software. Although the diffuser setup created a uniform light source, the first step was to mask out the pixels present in the background of the image. This was completed by calculating a gray threshold, above which (lighter gray values) data was eliminated, and below which data was

retained. From there, the position of the pixels denoting the boundary were resolved and used to estimate the four edges of the preform. Next, 8 equally spaced vertical and horizontal line profiles were extracted. Since there was no binder contained in the veil fibres, portions of the preform were vulnerable to displacement from their original positions. Clumps of veil fibres observed along the outer boundary of preforms were omitted from line profiles by selecting the middle 80% in length of all horizontal and vertical segments. Shown in Figure 4.3 is the preform from Figure 4.1 with indications of the image processing operations carried out. A sample line profile, centered about the mean gray value, is displayed in Figure 4.4.

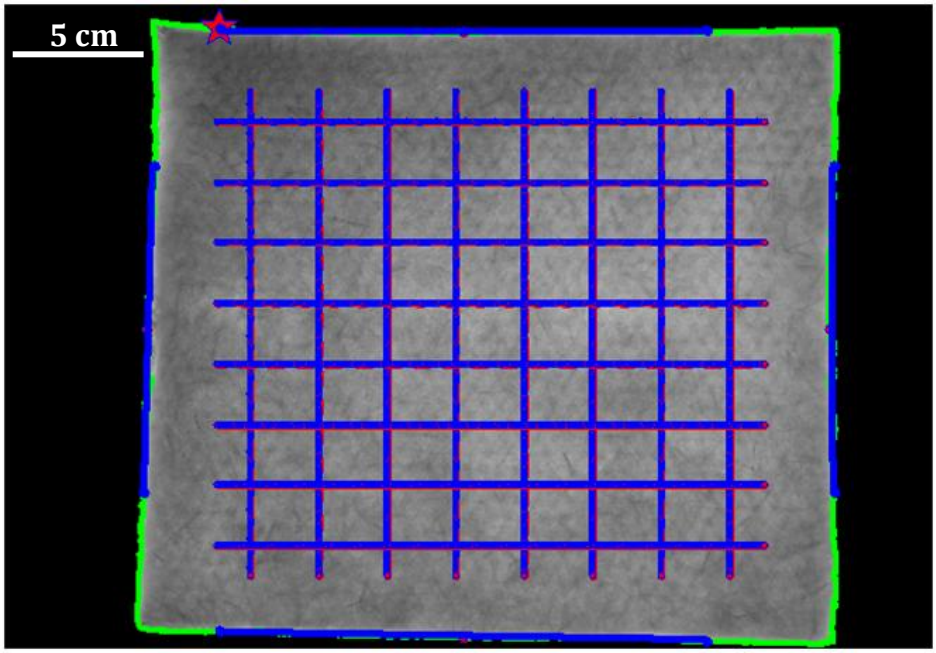

Figure 4.3: Image of preform from Set 2 (V_f = 14%, Top Veil wt% = 15%) with background masked out, boundaries and edges indicated, and vertical and horizontal line profiles drawn.

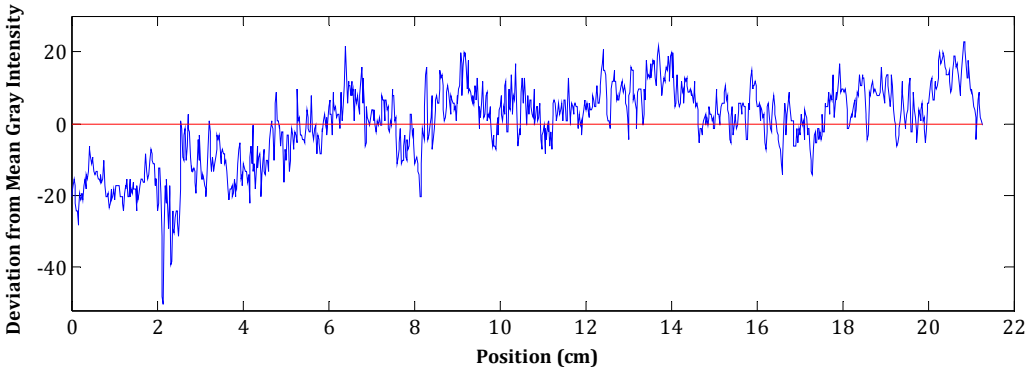

Figure 4.4: Line profile extracted from light transmission image of dry preform

Finally, the average grayscale roughness value, G_a, as described in Eq. 3.1, was calculated for each of the extracted line profiles. By determining the mean value of these 16 calculations, a number by which the various preforms could be compared was obtained. The custom MATLAB code implemented for this work returned average deviations from the mean ranging from 8.1516 to 10.0503 gray values, as shown in Figure 4.5. The lowest calculated values, and thus best results, belonged to (from best to worst) preform 8-1, 3-1 and 1-1, while the worst results were obtained for preform 2-2, 2-1, and 7-2. Within a set, the values obtained for each of the two cuts appear to be relatively close, thus indicating that preforms of similar architecture produce similar light transparency results.

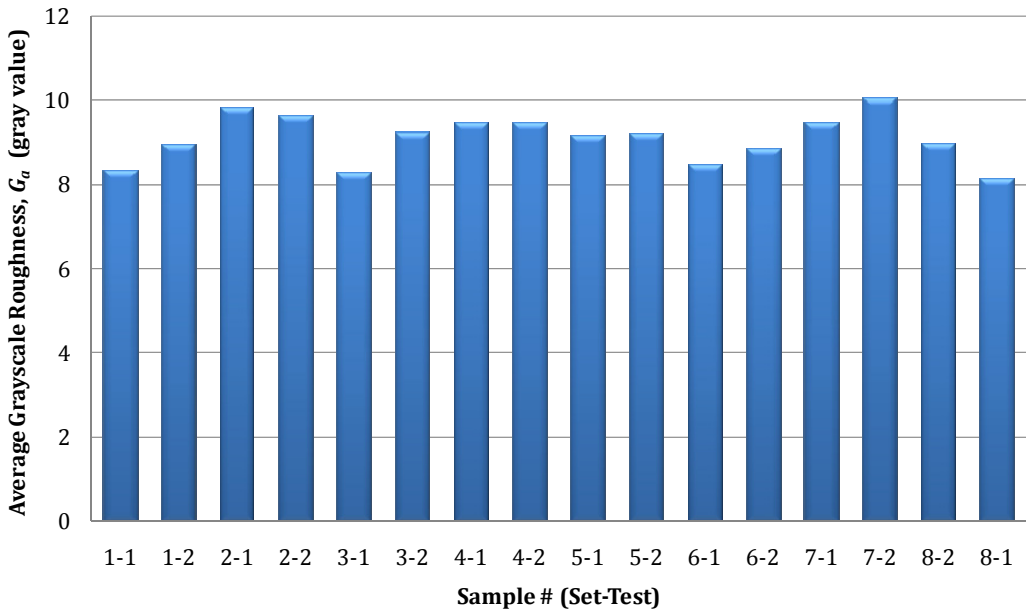

Figure 4.5: Bar chart of average grayscale roughness values for each sample

Grouping the data by veil weight fraction, and then plotting average grayscale roughness according to fibre volume fraction, gives Figure 4.6. Additionally, 3rd order polynomial trend lines for each group are presented. For the 10 wt% veil, an increasing trend is observed, while a decreasing trend is seen for the 15 wt% group. Also, within collections of similar volume fraction, there exists a large range of values, especially for the extreme values of 14% and 23% (areal densities of 1138 g/m^2 and 1870 g/m^2).

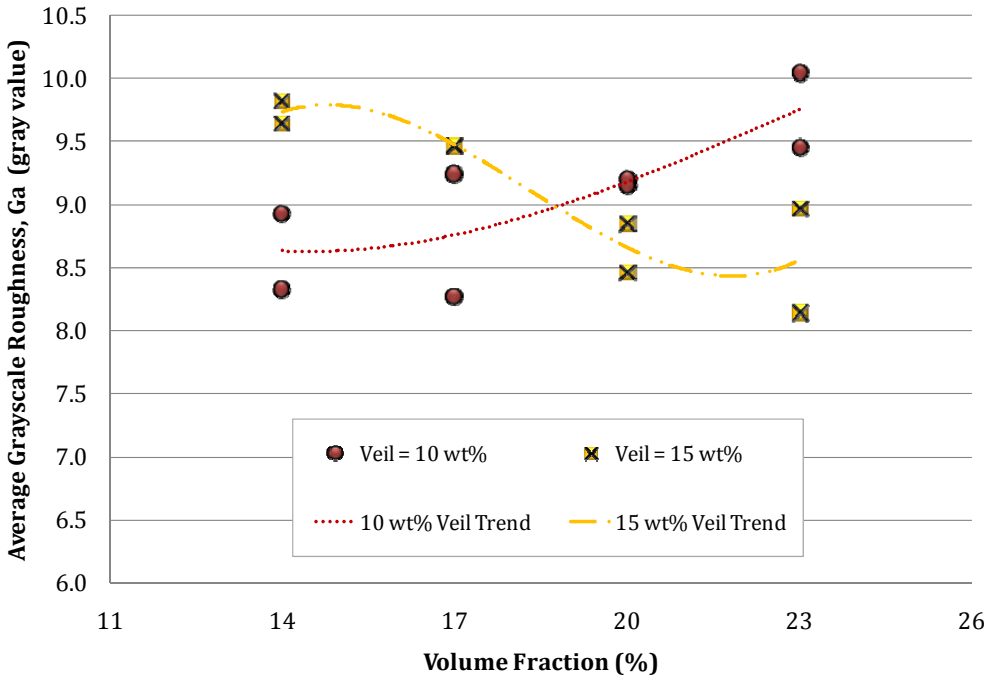

Figure 4.6: Plot of image analysis results – average grayscale roughness values plotted with respect to fibre volume fraction

4.2 Test Panels Manufactured by RTM

Composite panels fulfilling the entire L-8 test matrix required by the Taguchi method were manufactured by RTM with the task of maintaining identical injection parameters for all cases. Details regarding the RTM processing are presented in Section 4.2.1, with the typical cure development discussed in Section 4.2.2. The results obtained by visual inspection of the test panels are presented in Section 4.2.3.

4.2.1 RTM Processing

The process described in Section 3.4.1 was followed during the resin injection moulding of each test panel. A total of 16 test panels were manufactured according to a randomly generated order, as described in Table 4.1. Despite multiple cases where complications during the injection process caused inconsistencies in obtaining panels that had a glossy finish and were smooth throughout the entire moulded area, each of the samples contained regions that could be considered representative of the desired finish.

Table 4.1: Information regarding the RTM processing of each test panel

#	Set-Test	Areal Density (g/m^2)	TopVeil wt%	Injection Time (seconds)	Notes
1	4-1	1382	15	40	Tube leak @ 13 mins
2	3-1	1382	10	35	Tube leak @ 13 mins
3	6-1	1626	15	51	-
4	7-1	1870	10	41	Tube leak @ 13 mins
5	2-1	1138	15	34	Tube leak @ 13 mins
6	1-1	1138	10	52	-
7	---	1870	15	N/A	Part scrapped
8	---	1626	10	N/A	Part scrapped
9	3-2	1382	10	20	-
10	7-2	1870	10	21	-
11	1-2	1138	10	30	-
12	5-1	1626	10	30	-
13	8-1	1870	15	25	-
14	4-2	1382	15	25	Exit leak
15	2-2	1138	15	25	Exit leak
16	6-2	1626	15	22	-
17	8-2	1870	15	22	Release agent streaks
18	5-2	1626	10	21	Release agent streaks

RTM injections #7 and #8 were parts that needed to be scrapped due to incomplete infiltration of the fibreglass preforms. This was due to the calcium carbonate used as filler in the resin mixture, which ran out after six tests and was replaced by an older batch which had clearly undergone enough of a chemical change to limit the flow of the resin. For injections thereafter, a newly purchased batch of calcium carbonate was used, as evidenced by the lower time required for the resin to infiltrate the preform and flow out the exit.

In the case of injections #1, #2, #4, and #5, the use of polyethylene tubing incorrectly rated for the temperature and pressure needs of RTM processing led to a rupture in the inlet tubing at the 13 minute mark, corresponding to when the resin was undergoing volumetric expansion caused by the LPAs. Since preform infiltration was already complete, the effect was seen in the form of ripples or waviness on the finished panel, as opposed to dry sections. These defects, however, were limited to certain regions and did not appear to affect the rest of the panel, which exhibited the desired consistent and glossy finish. In a similar manner, incorrect sealing of the exit port caused leaks which produced the same regional ripples in injections #14 and #15. It should be noted that the situation regarding inadequate polyethylene tubing was rectified by replacing these components with a more robust set of nylon tubing.

In the case of injections #17 and #18, a saturated cloth used for the application and buffing of release agent caused streaks on the mould, which at the time were imperceptible, to produce streak marks on the finished panels. Again, these

defects were present only in certain areas, thus allowing for adequately sized representative regions to be obtained.

4.2.2 Typical Cure Development

As outlined in Section 3.4.2, the development of the RTM process was monitored by pressure and temperature sensors throughout the part curing. The test panels were left in the mould for 30 minutes with injection pressure applied at 621 kPa, and force applied by the hydraulic press. The top and bottom moulds were maintained at 75°C and 95°C by circulating warm water. Presented in Figure 4.7 is the data acquired from a typical cure cycle, in this case being that of injection #12, which produced panel 5-1. Data from all tests is presented in Appendix B.

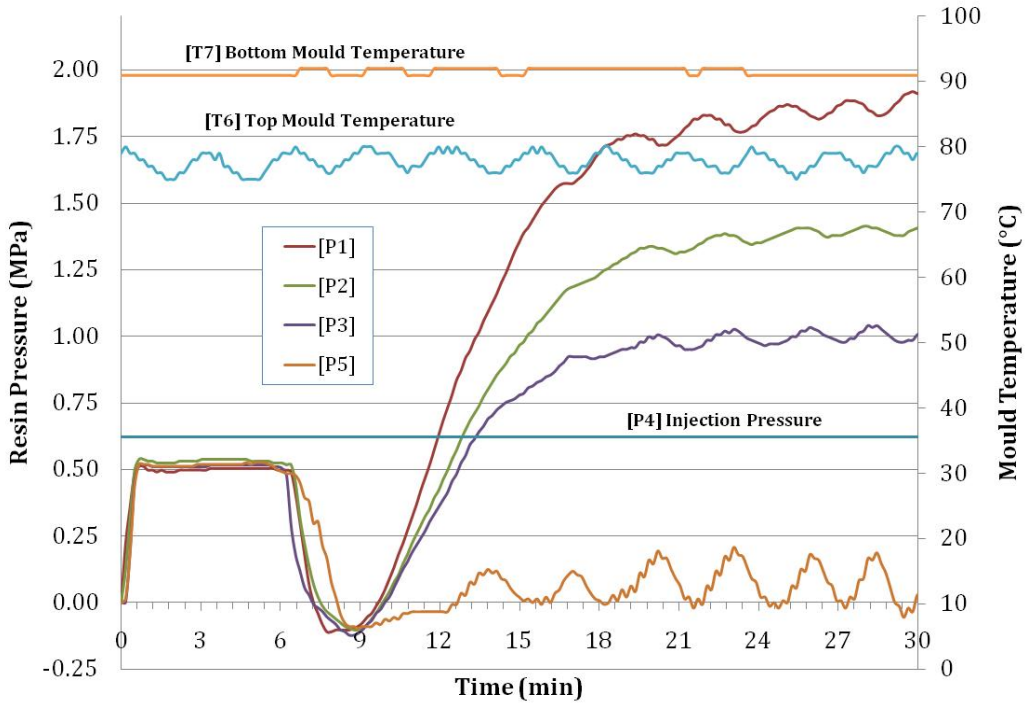

Figure 4.7: Typical pressure and temperature development during RTM processing

The plot shows the temperature maintained on the top and bottom moulds, though the curve is in a sinusoidal form. This is due to the warm water which was circulated into the moulds warm, cooled, and then replaced by new warm water approximately every 3 minutes. The four pressure sensors embedded into the moulds (as seen in Figure 3.5) measured the resin pressure throughout the cure development. The values were zeroed with the mould cavity closed and only the dry preform present. Upon injection, the pressure mounts to approximately 500 kPa and stays there for about 6 minutes, at which point resin volumetric shrinkage begins to set in. Work by Raja [5], observed that LPAs remained inactive until a degree-of-cure of approximately 0.5, following which expansion of the thermoplastic particles starts. This expansion is seen after about 9 minutes in the cure development shown in Figure 4.7, and continues until the resin pressure begins to level off after 20 minutes. Again, sinusoidal curves are seen and can be attributed to the circulating water, though this time in the case of the pressure values. As the resin pressure stabilizes, it is clear there is a cure gradient at different sensor locations. This phenomenon can be accounted for by the fact that the cure starts at the vent port and travels towards the injection port, as detailed by Raja [5]. It is of interest to note that rapid expansion of the resin is occurring at the 13 minute mark, which corresponds to the time when several of the injection tests had ruptures in the polyethylene tubing. It is evident that in addition to the elevated processing temperature, the internal pressure of nearly 1 MPa caused the tubing to break.

4.2.3 Visual Inspection of Surface Finish

With the objective of completing an initial investigation into the surface finish quality of the manufactured test panels, a method of visual inspection was employed. The region containing the most desirable surface finish within each panel was compared side by side with each of the others until an overall ranking was obtained. The decision of whether a panel was better or worse than another was based upon which one appeared to be more flat, smooth and exempt of undesirable waviness, as well as the desire to have a more mirror-like surface. Table 4.2 below categorizes the results and gives a description of the qualities observed within each category.

Table 4.2: Quality of surface finish observed in test panels

Quality	Test Panels	Description
Best	2-1, 6-1, 7-1	Glossy, mirror-like finish.
	6-2, 8-1, 5-1	Glossy finish.
Worst	2-2, 5-2, 8-2, 3-2, 1-1, 3-1, 7-2, 4-1, 1-2, 4-2	Semi-gloss finish.

In the case of the best panels, the fibre lattice pattern was clearly visible as an image on the surface, though the texture was not affected. Meanwhile, the image of the fibre lattice pattern was completely obscured in the worst panels.

It is interesting to note that, by observation, preforms within the same manufactured set (e.g. Set 2 & 7) provided samples falling in both the best and worst category of surface finish quality. One would expect preforms cut from the same sheet to output similar surface finish results if all other factors remained

constant. The possibility that the fibre areal density and surface veil thickness are weak factors contributing the surface finish quality appears to be the likely explanation for such results. Thus, even slight variations in dominant manufacturing factors such as injection pressure could have a larger effect on surface quality than variations in fibre areal density and surface veil thickness.

4.3 ONDULO Measurements

With the aim of gaining a more quantitative measure of the surface finish, each of the test panels was imaged using the ONDULO system, following which analysis was carried out utilising MountainsMap topography software. Obtained from this exercise were roughness values used to compare the quality of each finished test panel.

4.3.1 ONDULO Measurement System

The technique and parameters outlined in Section 3.5.1 were applied for the purpose of imaging each of the 16 test panels manufactured for this project. An image of test panel 6-1 is shown in Figure 4.8. As mentioned, the 16-mm lens provided a trapezoidal viewport of each panel due to the conical point-of-view of the digital camera. The area outside this viewport captured by the system is indicated as 'NM' – not measured. A noticeable gradient from light to dark appeared from the top to the bottom of the image. This is an artefact of the ONDULO technique that needed to be removed by the image processing software. The images appeared most clearly in the high-lustre regions, and

completely blacked out in the regions where light was not correctly reflected. Thus, black dots were seen in locations where the pressure and temperature sensors had left an imprint on the curing of the part. Additional defects were seen in the form of scratches, seen just to the left of centre, which were simply mirroring scratches that existed on the mould itself.

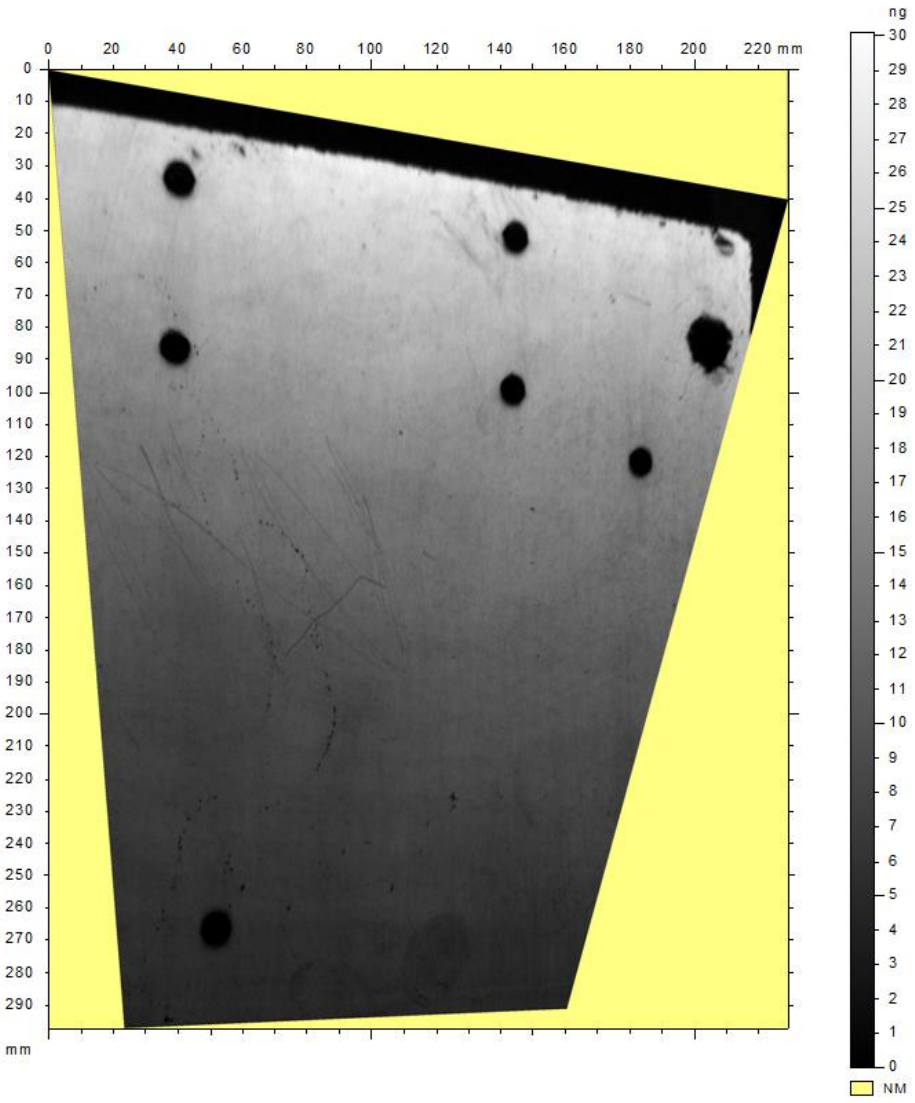

Figure 4.8: Image of test panel 6-1 acquired via the ONDULO system

4.3.2 MountainsMap Image Analysis

With the intention of analyzing the data acquired by the ONDULO system, DigitalSurf MountainsMap Topography XT software was employed to extract relevant data. A line profile evaluation length of 80 mm was selected based upon the ISO 12085 standard [24]. Thus, for the purposes of analysis, an area measuring 80 mm x 80 mm deemed 'best' was chosen as a representative sample for each test panel. These regions were then processed using a cubic spline filter with a low-pass cutoff of 8 mm. The filter was needed to remove the slight gradient in darkness due to the imaging of the phased pattern during the acquisition stage. Shown in Figure 4.9 is an ONDULO image of the representative sample area from test 6-1. Figure 4.10 shows the filtered image, devoid of the darkness gradient.

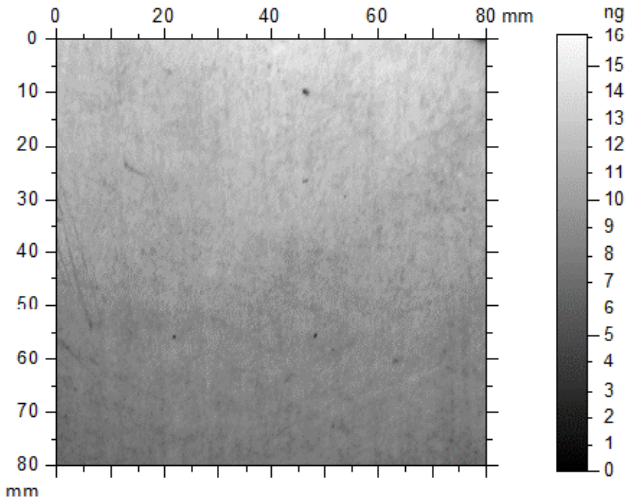

Figure 4.9: Image of 'best' region for sample 6-1 obtained from ONDULO system

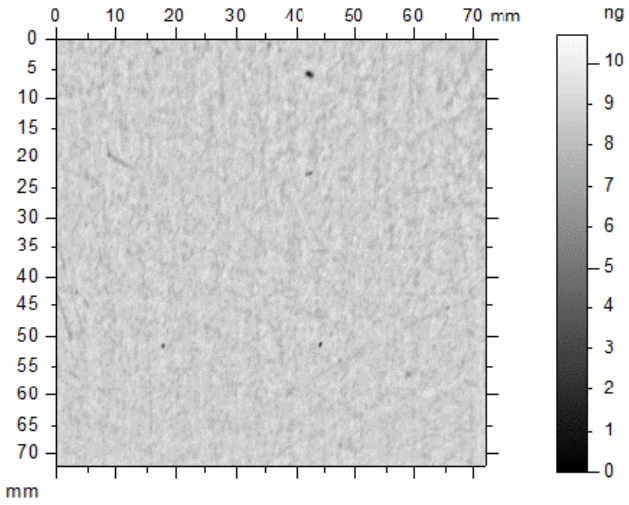

Figure 4.10: Image of 'best' region for sample 6-1 following application of cubic spline filtering

4.3.2.1 Omission of Defects

Despite making every effort to manufacture parts in exactly the same manner every time, a great deal of variability in the overall quality of parts remained. This was due to the complexity of the RTM process employed for this research, specifically the materials and tools used to carry out injections. Flow problems due to the loss of pressure at the inlet arose, resulting in ripples or waviness in the finished part at locations dependent on the moment and duration at which a leak may have occurred. Such flow problems occurred in samples 2-1, 2-2, 3-1, 4-1, 4-2, and 7-1. Also, scratches present on the mirror-like mould surface, or streaks remaining from the application of release agent (samples 5-2 & 8-2), would appear as imperfections on the finished test panels. The ONDULO imaging system is extremely effective at revealing defects that exists in composite parts, thus allowing for the undesirable regions to be omitted from the surface quality analysis. Shown in Figure 4.11, Figure 4.12, and Figure 4.13 are images

illustrating each of the discussed manufacturing defects, namely ripples, scratches, and streaks.

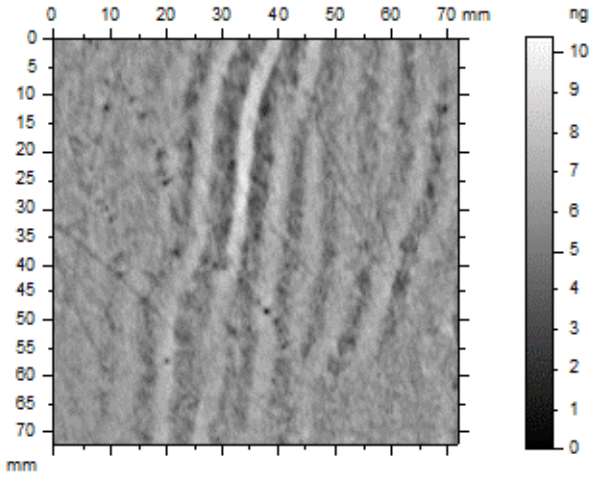

Figure 4.11: Image of ripples in finished part due to flow problems (panel 4-2)

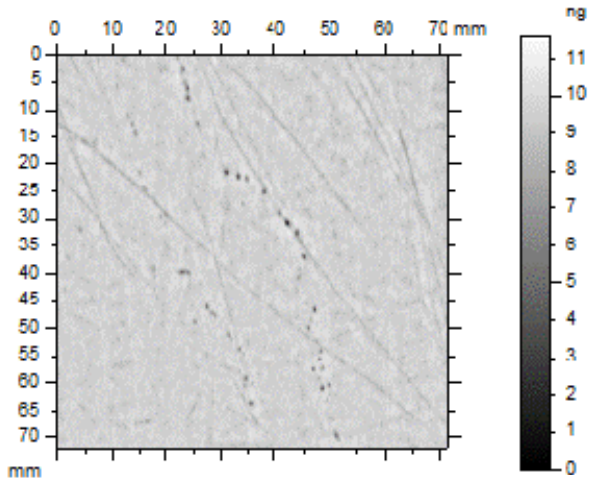

Figure 4.12: Image of marks mimicking scratches present on mould surface (panel 2-1)

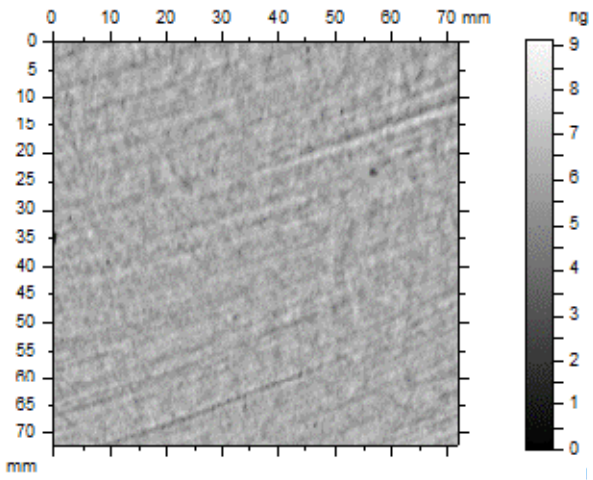

Figure 4.13: Image of streaks as a consequence of incorrect release agent application (panel 8-2)

4.3.3 Roughness Results

Having established the 'best' region measuring 80 mm x 80 mm for each test panel, the focus was next on calculating average roughness values. This was completed by first extracting 8 vertical and 8 horizontal line profiles from the given area. Although the system could not provide data accurately calibrated to a metric scale, the information acquired allowed for analysis using the grayscale intensity of pixels. According to the ISO 12085 standard, average roughness motif values can be calculated from the line profiles. The average roughness motifs calculated from vertical line profiles were consistently lower than that obtained from the horizontals, and thus the average of these two values is used as the metric for comparison. Figure 4.14 shows a sample line profile extracted from panel 2-1, while Figure 4.15 displays the average roughness motif profile obtained.

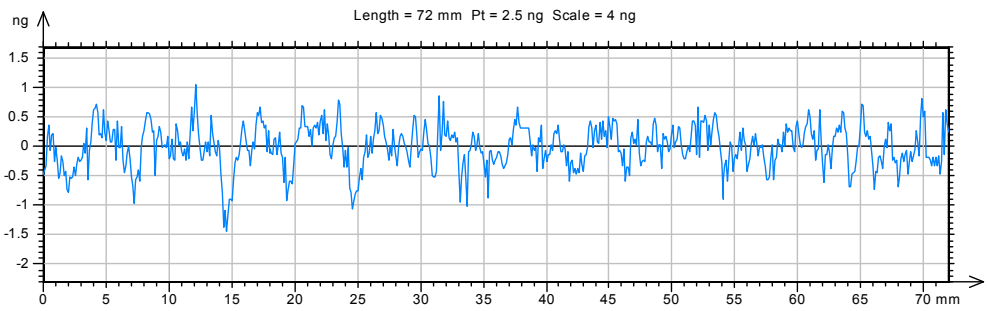

Figure 4.14: Line profile extracted from filtered 'best' region in test panel 2-1

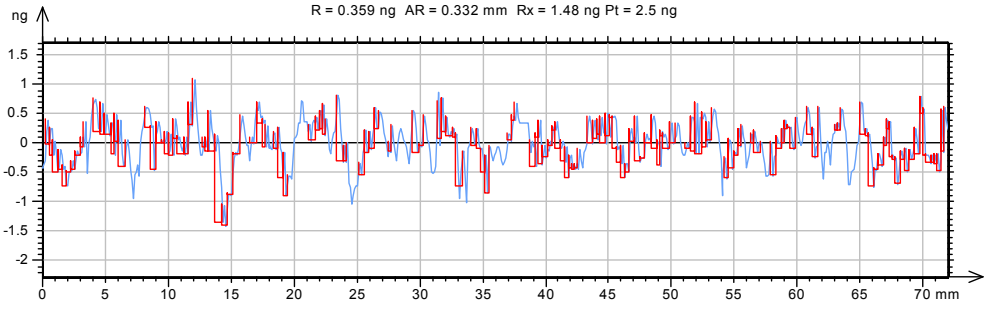

Figure 4.15: Roughness motif for line profile of filtered 'best' region in test panel 2-1

Shown in Figure 4.16, the results ranged from 0.234 to 0.413 pixels, with the best values seen in samples 6-2, 4-2, and 2-2, and worst in 8-1, 5-1, and 5-2. This value of grayscale pixel intensity, however, cannot be compared directly with that from the photographs of the dry preforms since each employs a different optical technique. The large variation indicated by the error bars can be explained by the discrepancy between the average vertical and horizontal values.

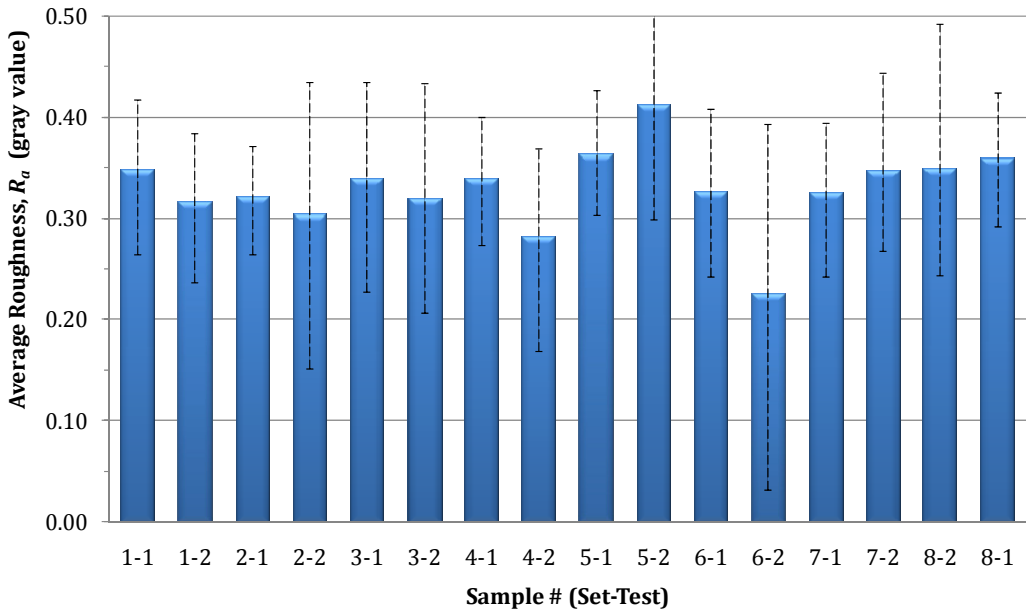

Figure 4.16: Bar chart of average roughness values from ONDULO for each sample

Figure 4.17 shows the average roughness motifs plotted according to fibre volume fraction. Again, sets are regrouped by surface veil weight fraction and 3rd order polynomial trend lines are included. All values except for those corresponding to the 20% fibre volume fraction are seen to be between 0.30 and 0.35 gray intensity. At the 20% mark, all four test panels appear to have produced very different results, with the larger veil wt% resulting in a smaller roughness and therefore better finish.

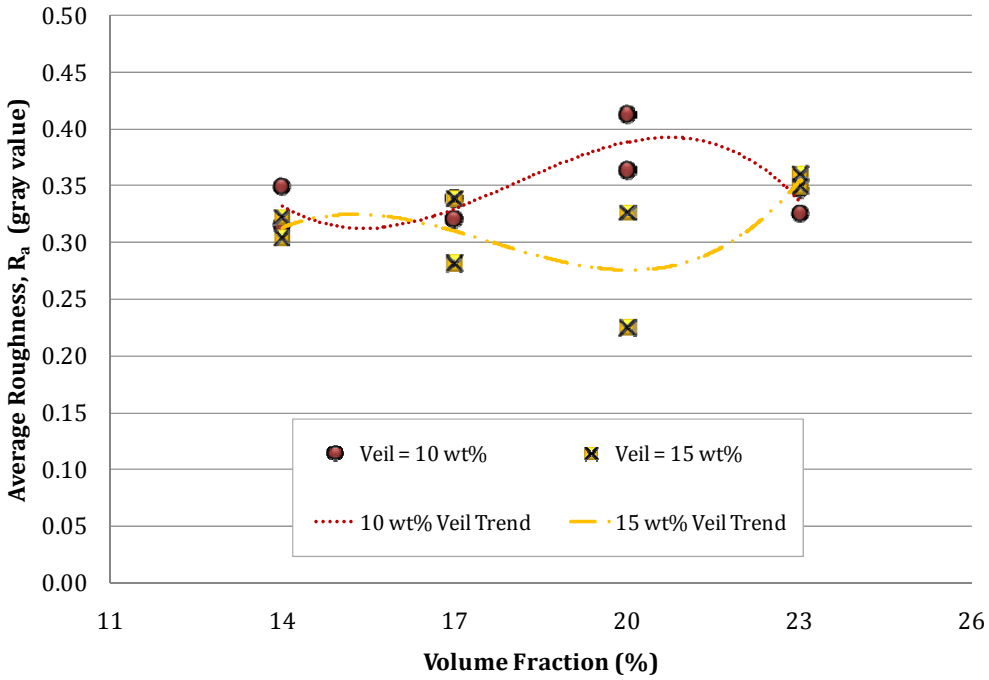

Figure 4.17: Plot of ONDULO results – average roughness values plotted with respect to fibre volume fraction

4.4 Analysis of Variance

Having compiled the results fulfilling the L-8 Taguchi experiment matrix, the goal was next to gain an understanding of the trends observed. Analysis of Variance (ANOVA) is the method employed with the Taguchi method in order to determine the relative influence and interactions between factors, as well as influence of experimental error. The Degrees-of-Freedom (DOF) for each factor were determined based on the number of levels studied, while the DOF for the experiment itself was established by the number of tests run. Further values, such as Sum-of-Squares, Variance, F-Ratio, and Pure Sum are statistical calculations based upon the quantitative results obtained.

4.4.1 Dry Preform Image Analysis

ANOVA was carried out based on the results obtained from the image analysis of the dry preforms. The influence of the fibre volume fraction was larger than that of the veil weight fraction; however, both were dwarfed by the influence of the error term of the experiments, as seen in Table 4.3. The minimum MSD would imply that Set 8 (V_f = 23%, Veil wt% = 15%) is the optimal condition, while the trends within each factor would point to Set 5 (V_f = 20%, Veil wt% = 10%) as the optimal configuration.

Table 4.3: ANOVA for image analysis data, based on design factors

#	**Preform V_f**	**Veil W_f**	**Error**	**Total**
Factor DOF (f)	3	1	11	15
Sum of Squares (S)	0.169	0.003	4.659	4.831
Variance (V)	0.056	0.003	0.424	0.322
F-Ratio (F)	0.133	0.006	-	-
Pure Sum (S')	-1.1	-0.42	-	-
Percent Influence (P)	0%	0%	100%	100%

4.4.2 ONDULO Measurements

Similarly, the ANOVA for the results obtained from the ONDULA system showed that the error term has a dominant influence on the experiment. The veil thickness represented 11% of the influence, while the fibre volume fraction had no influence, and the error/other factors filled the remaining 89%. A slight increase in roughness was observed as fibre volume fraction was increased, and veil size is decreased. Thus, the optimal conditions according to ANOVA are seen in Set 4 (V_f = 17%, Veil wt% = 15%), while the minimum MSD occurs in Set 6

(V_f = 20%, Veil wt% = 15%). Table 4.4 displays the ANOVA results according to the design factors studied in this experiment.

Table 4.4: ANOVA for ONDULO data, based on design factors

#	**Preform V_f**	**Veil W_f**	**Error**	**Total**
Factor DOF (f)	3	1	11	15
Sum of Squares (S)	0.002	0.004	0.018	0.024
Variance (V)	5E-04	0.004	0.002	0.002
F-Ratio (F)	0.318	2.6	-	-
Pure Sum (S')	0	0.003	-	-
Percent Influence (P)	0%	11%	89%	100%

4.4.3 Discussion of ANOVA Results

Although the use of ANOVA has allowed for the determination of 'optimal conditions', it is apparent that the variability over the range of fibre volume fractions and surface veil weight fractions play a very slight role in the quality of a composite part's surface finish. In the process of manufacturing these parts, a certain intuition regarding the influence of various factors was developed thanks to the hands-on experience gained. The error term included in the ANOVA combines all uncontrollable and excluded factors, as well as any experimental error. Thus, when the error represents an extremely large percent influence in the experiment, it means that the process is too sensitive to the influence of uncontrollable factors and the samples have a large inherent variability [21]. Based upon the chosen evaluation technique, the results obtained indicate that fibre volume fraction and surface veil thickness have little to no influence on the surface finish quality.

4.5 Correlation of Results

One of the main objectives of this work was to determine the relationship between quality of fibreglass preforms and surface finish of test panels manufactured by RTM. By observing the large disparity between the set rankings of surface quality for each of the two methods, it is evident that there is no apparent relationship between the results obtained from the image analysis and those from the ONDULO system. One would expect the best results from the image analysis to correspond to the moulded samples with the best surface finish in order for a correlation to be drawn. This is not seen either by observation or using the ONDULO measurement technique. The implication is that although the analysis carried out in both cases may be acceptable, no conclusions can be drawn prior to moulding with respect to the ability to predict which preforms will result in superior surface quality.

5 Conclusions

The goal of this work was to study the effect of preform variability on the surface finish of Class A composite parts manufactured by RTM. This was accomplished by first determining preform characteristics of interest, then by establishing a set of experiments which allowed for the investigation of variability. Next, the quality of dry preforms was studied both prior to, and following RTM processing. Finally, ANOVA was employed to understand the influence of the factors studied.

The following details, as they pertain to the initial objectives of this project, can be concluded upon:

1. Preform characteristics: Although F3P preform material selection and machine parameters are of interest, fibreglass areal density and top veil weight fraction were selected for further study. A range of 1138 g/m^2 to 1870 g/m^2 was chosen for areal density, while 10 wt% and 15 wt% top veils were also picked for study.
2. Qualify dry preforms: A novel technique whereby the light transmitted through dry preforms is photographed was utilised. Acquired images were analysed in order to obtain average grayscale roughness values which quantified the consistency of the preform surface.
3. Surface finish characterisation: Composite test panels were manufactured by RTM, following which surface finish was characterised. This was completed first by visual inspection, then by making use of the ONDULO surface measurement system.

4. Relate results to surface finish: The results of the Taguchi method, according to ANOVA, demonstrated that surface finish quality is dominated by factors other than fibre areal density and surface veil thickness. No relation was observed between the quality of the preforms prior to and following moulding.

Based on the experimental techniques employed, the findings in this thesis suggest that small variations in preform fibre volume fraction and top veil thickness have no significant effect on the surface finish of 'Class A' composites parts manufactured by RTM.

5.1 Future Work

Further work is required to verify the accuracy of the optical methods used for imaging prior to and following moulding. The results obtained from a contact profilometer could be compared to the ONDULO results to determine to what extent the fibre lattice visible in the surface veil actually affects surface finish.

Also, it is of interest to study the average roughness motifs obtained within several different ranges of wavelengths to verify that the appropriate waviness components have been removed from the surface texture profiles.

Finally, it is of interest to understand the importance of micro-structural elements in the fiberglass preform. The effect of the lattice patterns included on the Class A side of the preforms, as well as the diameter and length of fibres should be addressed in order to qualify their contribution to surface finish.

6 References

[1] Tucker, N., Lindsey, Kevin, 2002, An Introduction to Automotive Composites, Rapra Technology Limited, Shawbury, U.K.

[2] Palardy, G., 2007, "Resin Volumetric Changes and Surface Finish Characterization of Composite Automotive Panels," Master's Thesis McGill University, Montréal, Qc.

[3] Black, S., 2008, "High-Volume Preformance for Automotive Application," Gardner Publications Inc.

[4] Potter, K., 1997, Resin Transfer Moulding, Chapman & Hall.

[5] Raja, M. H., 2005, "Experimental Optimization of Process Parameters to Obtain Class a Surface Finish in Resin Transfer Molding Process," PhD Thesis McGill University, Montreal, Qc.

[6] Wood, K., 2008, "Automotive Composites: Taking Subjectivity out of Class a Surface Evaluation," Composites Technology.

[7] Karbhari, V. M. S., S.G.; Steenkamer, D.A.; Wilkins, D.J., 1992, "Effect of Material, Process, and Equipment Variables on the Performance of Resin Transfer Moulded Parts," Composites Manufacturing, 3(3), pp. 143-152.

[8] Dutiro, C., 1995, "Factors Affecting Surface Finish of Rtm Products," MSc(Eng.) Imperial College of Science and Technology and Medicine, UK.

[9] Dutiro, C. A., R.N., 1997, "Factors Controlling Surface Finish in Resin Transfer Molding," SAMPE Journal, 33(5), pp. 19-23.

[10] Bayldon, J. M., 1996, "An in-Depth Study of Surface Finish in Resin Transfer Moulding," MSc(Eng.) Imperial College of Science and Technology and Medicine.

[11] Palardy, G.; Hubert, P.; Haider, M.; Lessard, L., 2008, "Optimization of Rtm Processing Parameters for Class a Surface Finish," Composites: Part B, 39(pp. 1280-1286.

[12] Palardy, G., Hubert, P., 2007, "Effect of Painting Process on the Surface Finish of Rtm Composite Car Body Panels," Paris, France.

[13] Haider, M., Hubert, P.; Lessard, L., 2007, "Cure Shrinkage Characterization and Modeling of a Polyester Resin Containing Low Profile Additives," Composites: Part A, 38(pp. 994-1009.

[14] Devries, J. E., 2007, "Title," Wayne State University.

[15] Chavka, N. G. D., J.S., Kleven, E.D., 2001, "F3p Fiber Preforming for the Aston Martin Vanquish," Proc. 2001 SAMPE Europe Int'l Conference, Paris.

[16] Harper, L. T. T., T.A.; Warrior, N.A.; Dahl, J.S.; Rudd, C.D., 2006, "Characterisation of Random Carbon Fibre Composites from a Directed Fibre Preforming Process: Analysis of Microstructural Parameters," Composites: Part A, 37(pp. 2136-2147.

[17] Dahl, J. D., M.; Steenmaker, D., 2004, "Processing and Performance of Chopped, Glass-Fiber-Reinforced Rtm Composites."

[18] Bebamzadeh, A. A., A.R.A.; Haukaas, T.; Vaziri, R.; Poursatip, A., 2005, "Probabilistic and Sensitivity Analysis of Surface Waviness of Rtm Manufactured Automotive Body Parts."

[19] Personal Communication with Kendall, K., Aston Martin.

[20] Fisher, R. A., 1993, Statistical Methods, Experimental Design, and Scientific Inference, Oxford University Press, Oxford, U.K.

[21] Roy, R. K., 2001, Design of Experiments Using the Taguchi Approach: 16 Steps to Product and Process Improvement, Wiley-Interscience, USA.

[22] Ansi/Asme, 1985, "B46.1: Surface Texture, Surface Roughness, Waviness and Lay."

[23] Mainsah, E. G., J.A.; Chetwynd, D.G., 2001, Metrology and Properties of Engineering Surfaces, Kluwer Academic Publishers, The Netherlands.

[24] Digitalsurf, 2008, "Mountainsmap: User Help Manual."

[25] Whitefield, R. J., "Non-Contact Optical Profilometer," Applied Optics, 14(10), pp. 2480-2485.

[26] Vorburger, T. V. R., J., 1990, Surface Finish Metrology Tutorial, Gaithersburg, MD.

[27] Techlab, 2002, Ondulo: L'analyse De L'aspect De Surface - Manuel D'utilisation, Metz, France.

[28] Debolt, M. A., 2004, "Surface Finish Evaluation Method for Class a Composite Substrates."

[29] Iso, "Surface Texture: Profile Method - Rules and Procedures for the Assessment of Surface Texture."

[30] Schubel, P. J. W., Nicholas A.; Kendall, Kenith N.; Rudd, Chris D., 2006, "Characterisation of Thermoset Laminates for Cosmetic Automotive Applications: Part I - Surface Characterisation," Composites: Part A, 37(pp. 1734-1746.

[31] Gan, M., "Understanding and Improving the Performance of Advanced Composites through Modelling the Effect of Material Variability."

7 Appendix A

7.1 Custom MATLAB Image Analysis Code

areal_density.m

```
% areal_density.m -- by Ronnie Lawand
% ------------------------------------------------
% Used to analyse fiberglass preform images

clc; clear all; close all;

fprintf('\n');
fprintf('PREFORM IMAGE ANALYSIS\n');
fprintf('----------------------\n');
fprintf(' Ronnie Lawand - 2009 \n');
fprintf('----------------------\n');
fprintf('\n');
fprintf('## -- File Name    --    Scale     Rough \n');

% Import image, convert to grayscale
[N, T] = xlsread('list.xlsx');
Text = cellstr(T);

Set8 = Text(:,4);
Images = [Set8];

% Show plots? -- No: for batch runs
print = 1;

for pic = 1:length(Images)

   clear vLP hLP
   File = char(Images(pic));
   rgb = imread(File);
   if print==0 fprintf('%2.0i -- %s -- ',pic,char(Images(pic))); end

   % Convert to gray, create binary image
   gray = rgb2gray(rgb);
   level = graythresh(gray);
   bin = ~im2bw(gray,level);

   % Determine an initial point, find boundary
   dim = size(bin);
   col = round(dim(2)/4);
   row = find(bin(:,col),1);
   boundary = bwtraceboundary(bin,[row, col],'E');

   % Masked images of preform and background
```

```
   bipreform = roipoly(gray,boundary(:,2),boundary(:,1));
   preform = immultiply(gray,bipreform);
%     mask1 = immultiply(gray,~bipreform);
%     background = immultiply(mask1,~bin);

   % Show binary image and boundary of preform
   if print==1
      figure1=figure;
      imshow(preform);
      hold on;
      plot(boundary(:,2),boundary(:,1),'g','LineWidth',3);
      plot(col,row,'MarkerFaceColor','r','MarkerSize',20,'Marker','pentagram');
   end



   % \\\\\\\\\ DETERMINE LINE PROFILE \\\\\\\\\

   % Determine and plot each of the column lines
   for c = 1:3
      cLP_col(c) = round(dim(2)*c/4);                    % Picks column to use
      cLP_start(c) = find(bin(:,cLP_col(c)),1,'first');   % Finds start of column
      cLP_end(c) = find(bin(:,cLP_col(c)),1,'last');      % Finds end of column
      if print==1
         plot(cLP_col(c),cLP_start(c),'MarkerFaceColor','r','MarkerSize',5,'Marker','o');
         plot(cLP_col(c),cLP_end(c),'MarkerFaceColor','r','MarkerSize',5,'Marker','o');
      end
   end

   % Determine and plot each of the row lines
   for r = 1:3
      rLP_row(r) = round(dim(1)*r/4);
      rLP_start(r) = find(bin(rLP_row(r),:),1,'first');
      rLP_end(r) = find(bin(rLP_row(r),:),1,'last');
      if print==1
         plot(rLP_start(r),rLP_row(r),'MarkerFaceColor','r','MarkerSize',5,'Marker','o');
         plot(rLP_end(r),rLP_row(r),'MarkerFaceColor','r','MarkerSize',5,'Marker','o');
      end
   end

   vFirst = round(mean(cLP_start));
   vLast = round(mean(cLP_end));
   vLength = vLast - vFirst;       % Can be used for approximate sizing (vertical)
   hFirst = round(mean(rLP_start));
   hLast = round(mean(rLP_end));
   hLength = hLast - hFirst;       % Can be used for approximate sizing (horizontal)


   vx = round(hFirst+hLength*(0.15:0.1/1:0.85));
   vy = vFirst+round(vLength*0.1):vLast-round(vLength*0.1);
   for i = 1:length(vx)
      for j = 1:length(vy)
         if print==1 plot(vx(i),vy(j),'MarkerFaceColor','r','MarkerSize',2,'Marker','o'); end
         vLP(j,i) = preform(vy(j),vx(i));
      end
   end
```

```
hy = round(vFirst+vLength*(0.15:0.1/1:0.85));
hx = hFirst+round(hLength*0.1):hLast-round(hLength*0.1);
for i = 1:length(hy)
   for j = 1:length(hx)
      if print==1 plot(hx(j),hy(i),'MarkerFaceColor','r','MarkerSize',2,'Marker','o'); end
      hLP(j,i) = preform(hy(i),hx(j));
   end
end

clear dvLP
dvLP = double(vLP);
dhLP = double(hLP);

% ///////// DETERMINE LINE PROFILE /////////



% \\\\\\\\\ FIND PREFORM EDGES \\\\\\\\\
pt(1,:) = [cLP_start(1),cLP_col(1)];
pt(2,:) = [cLP_start(3),cLP_col(3)];
pt(3,:) = [rLP_row(1),rLP_end(1)];
pt(4,:) = [rLP_row(3),rLP_end(3)];
pt(5,:) = [cLP_end(3),cLP_col(3)];
pt(6,:) = [cLP_end(1),cLP_col(1)];
pt(7,:) = [rLP_row(3),rLP_start(3)];
pt(8,:) = [rLP_row(1),rLP_start(1)];

for i = 1:8
   edge_pts(i) = findbpt(pt(i,:),boundary);
   if print==1 plot(pt(i,2),pt(i,1),'MarkerFaceColor','b','MarkerSize',5,'Marker','o'); end
end

s = 1;
for i=1:4:5
   x = boundary(edge_pts(i):edge_pts(i+1),2);
   y = boundary(edge_pts(i):edge_pts(i+1),1);
   p = polyfit(x,y,1);
   slopes(s,:) = p;
   s = s+1;
   yp = p(1)*x+p(2);
   if print==1 plot(x,yp,'LineWidth',4); end
   clear x y p yp;
end

for i=3:4:7
   x = boundary(edge_pts(i):edge_pts(i+1),2);
   y = boundary(edge_pts(i):edge_pts(i+1),1);
   p = polyfit(y,x,1);
   slopes(s,:) = p;
   s = s+1;
   xp = p(1)*y+p(2);
   if print==1 plot(xp,y,'LineWidth',4); end
   clear x y p xp;
end
```

```
DSlopes = atand(slopes(:,1));
AvgHSlopes = mean(DSlopes(1:2));
AvgVSlopes = mean(DSlopes(3:4));

hPix = round(hLength*cosd(AvgHSlopes));
vPix = round(vLength*cosd(AvgVSlopes));
hcmpix = 26/hPix;
vcmpix = 24/vPix;
CMpPIX = (hcmpix+vcmpix)/2;

if print==1
   fprintf('Scale: %5.5f cm/pixel\n',CMpPIX);
   fprintf('\n');
else
   fprintf('  %5.5f  ',CMpPIX);
end


% ///////// FIND PREFORM EDGES /////////


% \\\\\\\\\ PLOT LINE PROFILES \\\\\\\\\

for i = 1:length(dvLP)
   dvLPx(i) = (i-1)*CMpPIX;
end
for i = 1:length(dhLP)
   dhLPx(i) = (i-1)*CMpPIX;
end

%    figure2=figure;
%    plot(dvLPx,dvLP);
%    plot(dhLPx,dhLP);


aaa = 5;
Avg_dhLP = mean(dhLP);
Avg_dvLP = mean(dvLP);

clear Dev_dvLP Dev_dhLP

for i = 1:8
   Dev_dvLP(:,i) = dvLP(:,i)- Avg_dvLP(i);
   Dev_dhLP(:,i) = dhLP(:,i)- Avg_dhLP(i);
end

figure3=figure;
plot(dhLPx,dhLP(:,aaa));
line([dhLPx(1),dhLPx(length(dhLPx))],[Avg_dhLP(aaa),Avg_dhLP(aaa)],'Color','r')

figure4=figure;
plot(dhLPx,Dev_dhLP(:,aaa));
line([dhLPx(1),dhLPx(length(dhLPx))],[0,0],'Color','r')

% ///////// PLOT LINE PROFILES /////////
```

```
    % \\\\\\\\\ ROUGHNESS VALUES \\\\\\\\\

    vR = mean(abs(Dev_dvLP));
    hR = mean(abs(Dev_dhLP));
    Rough = mean([vR,hR]);

    if print==1
        fprintf('Average Roughness: %5.4f gray values\n',Rough);
        fprintf('\n');
    else
        fprintf('  %5.4f  \n',Rough);
    end

    % ///////// ROUGHNESS VALUES /////////


end
```

findbpt.m

```
function pos = findbpt(pt,b)

d = 10000;

for i = 1:length(b)
    if b(i,:) == pt
        pos = i;
        break;
    else
        db = sqrt((abs(b(i,1)-pt(1)))^2 + (abs(b(i,2)-pt(2)))^2);
        if db<d
            d = db;
            pos = i;
        end
    end
end

end
```

8 Appendix B

Note: See Table 4.1 for complete information regarding the RTM processing of each test panel.

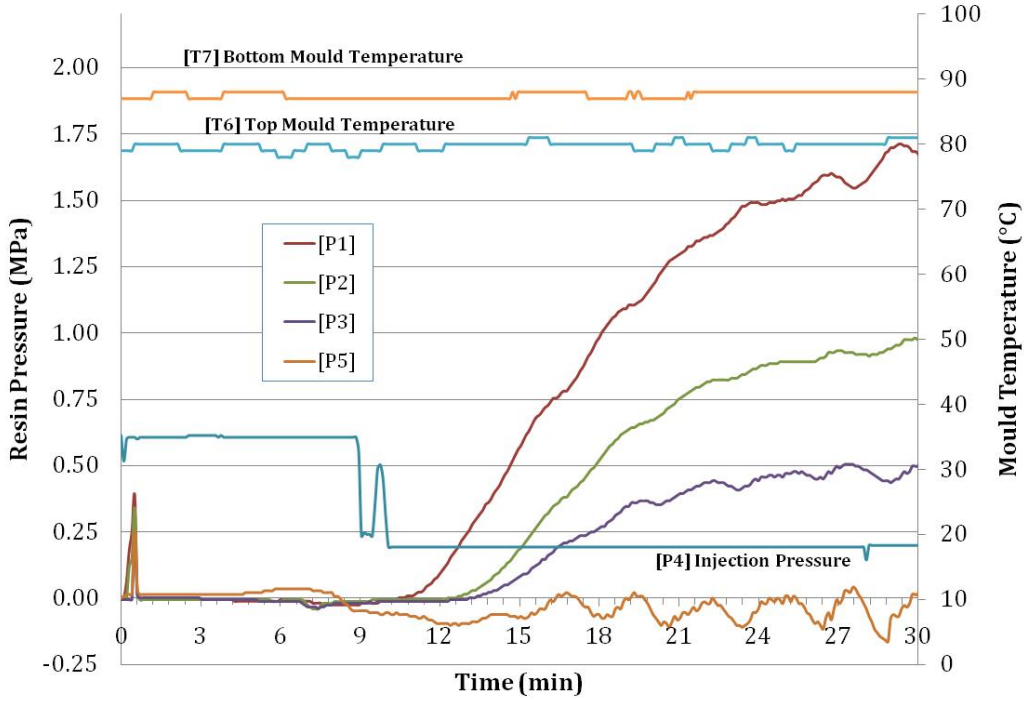

Figure 8.1: Pressure and temperature development during RTM injection #1 (test panel 4-1)

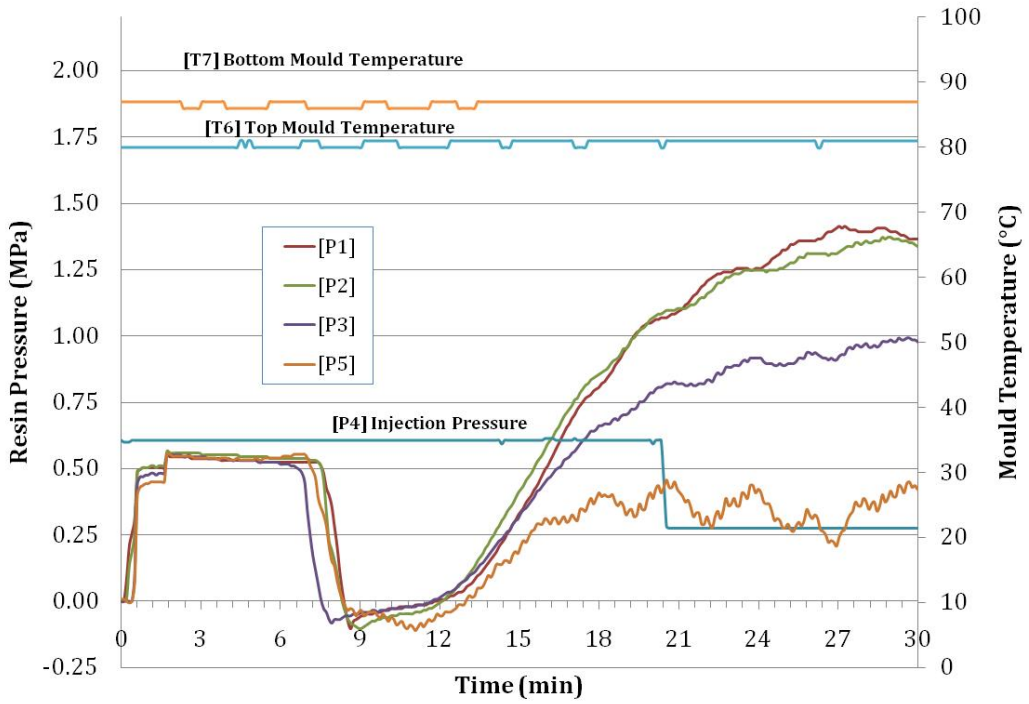

Figure 8.2: Pressure and temperature development during RTM injection #2 (test panel 3-1)

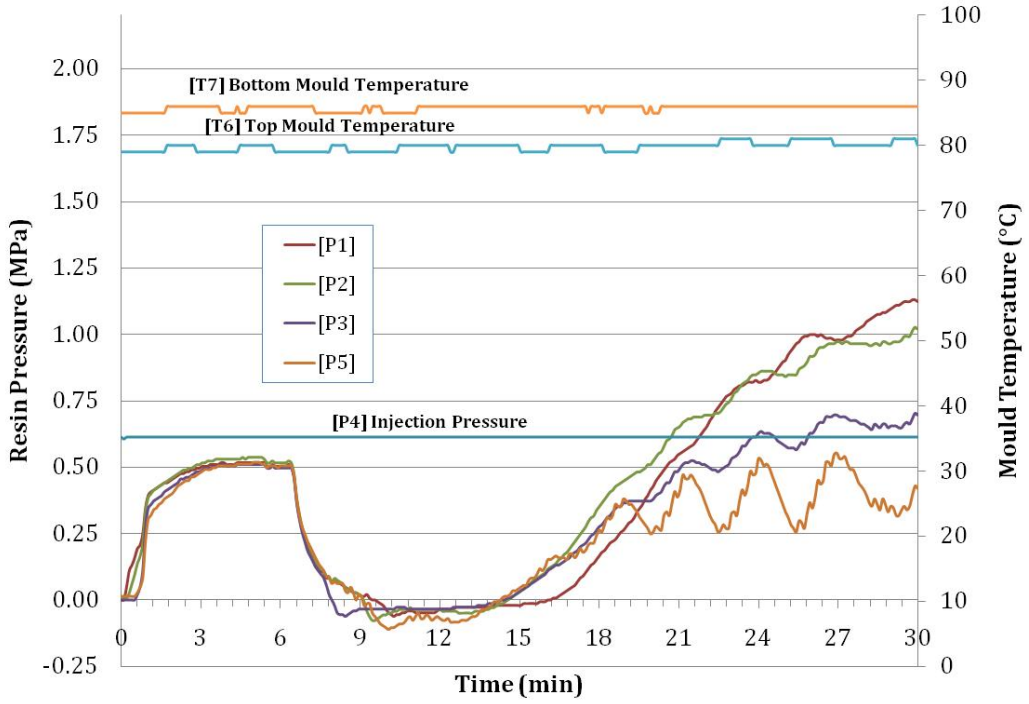

Figure 8.3: Pressure and temperature development during RTM injection #3 (test panel 6-1)

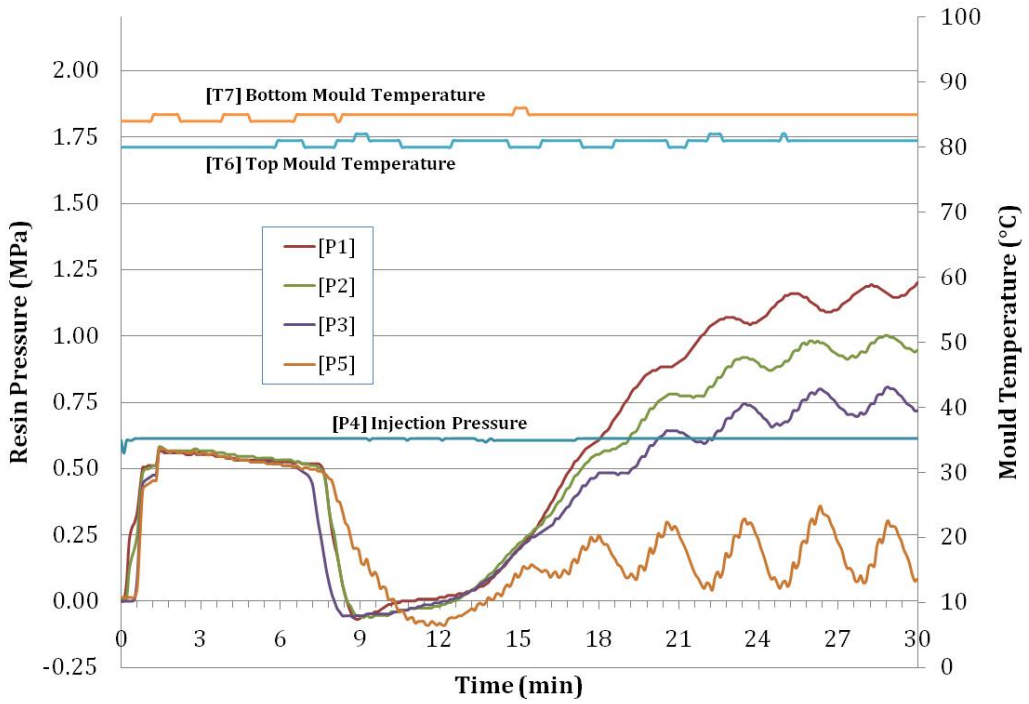

Figure 8.4: Pressure and temperature development during RTM injection #4 (test panel 7-1)

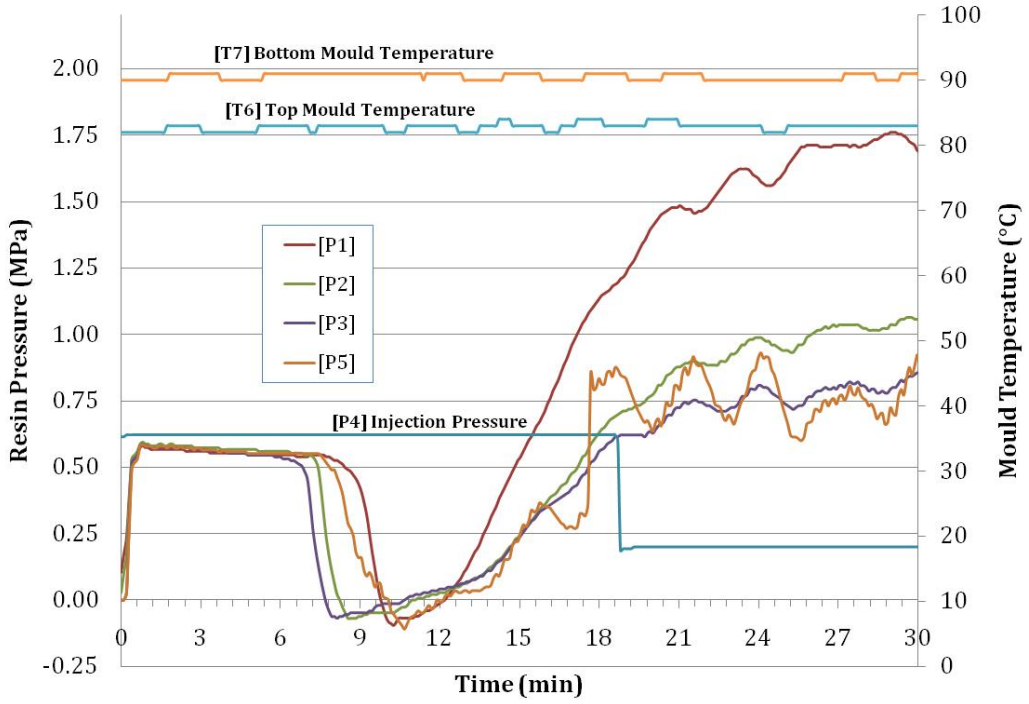

Figure 8.5: Pressure and temperature development during RTM injection #5 (test panel 2-1)

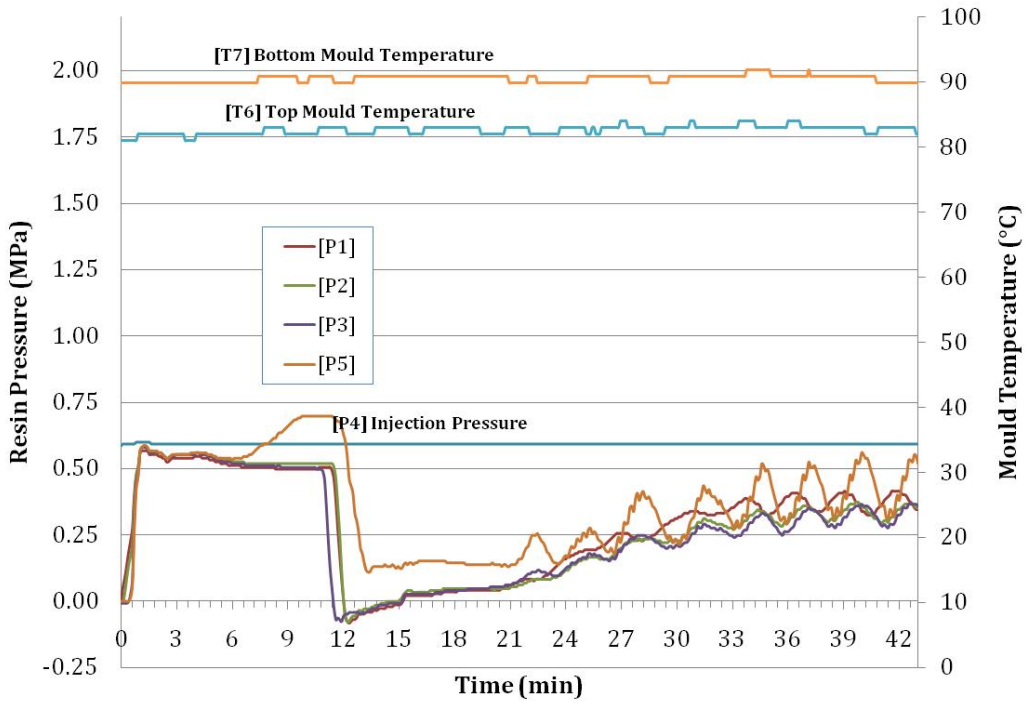

Figure 8.6: Pressure and temperature development during RTM injection #6 (test panel 1-1)

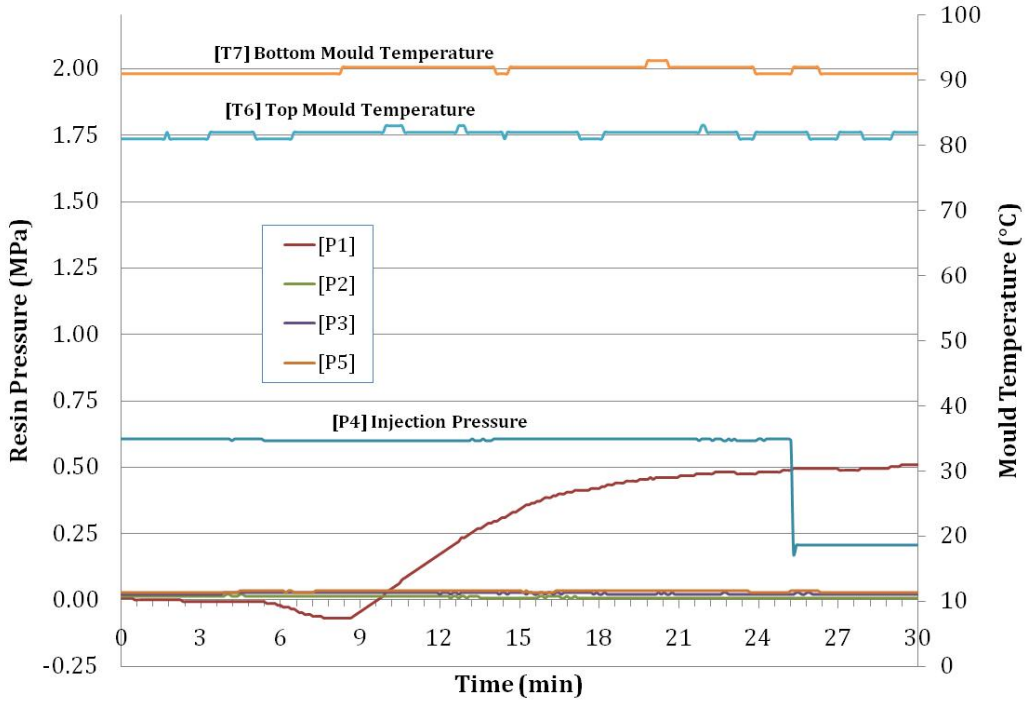

Figure 8.7: Pressure and temperature development during RTM injection #7 (part scrapped)

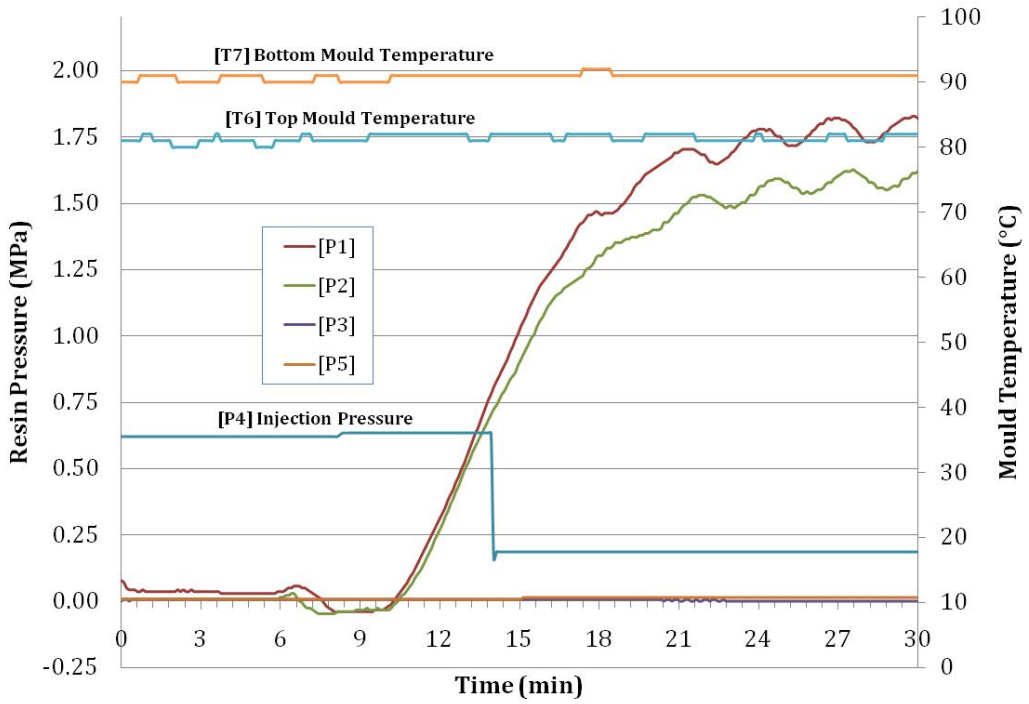

Figure 8.8: Pressure and temperature development during RTM injection #8 (part scrapped)

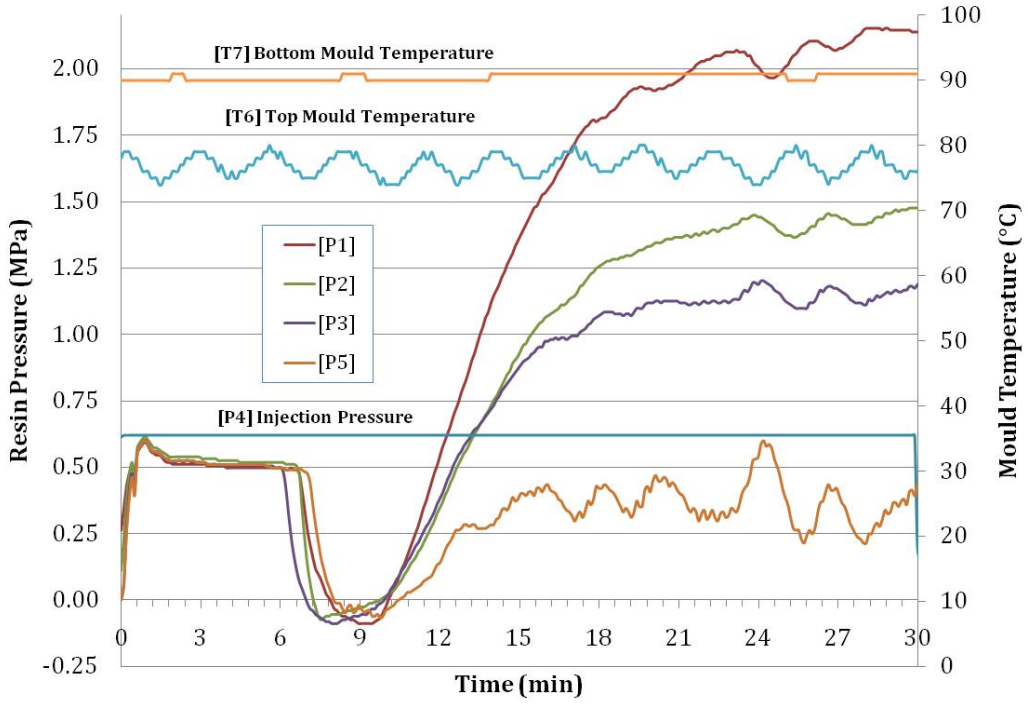

Figure 8.9: Pressure and temperature development during RTM injection #9 (test panel 3-2)

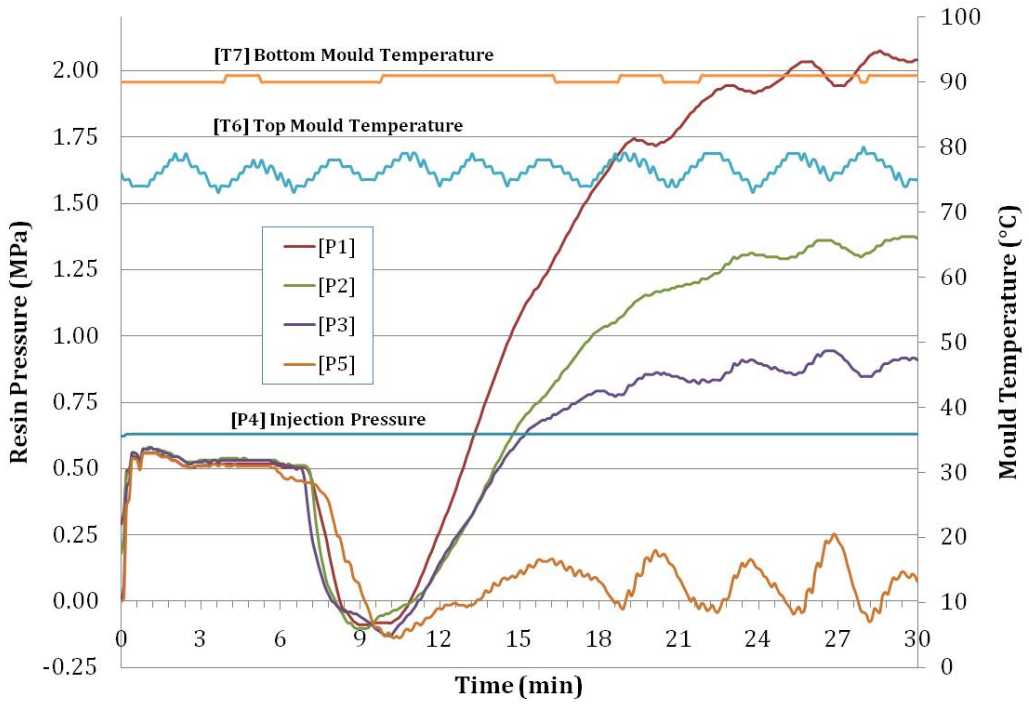

Figure 8.10: Pressure and temperature development during RTM injection #10 (test panel 7-2)

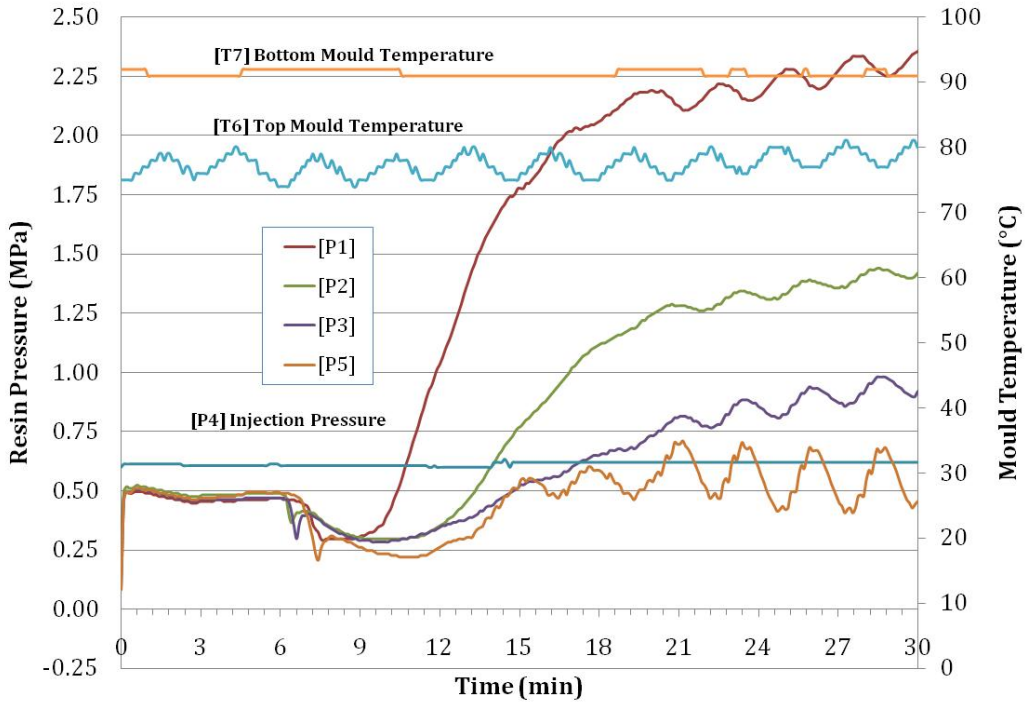

Figure 8.11: Pressure and temperature development during RTM injection #11 (test panel 1-2)

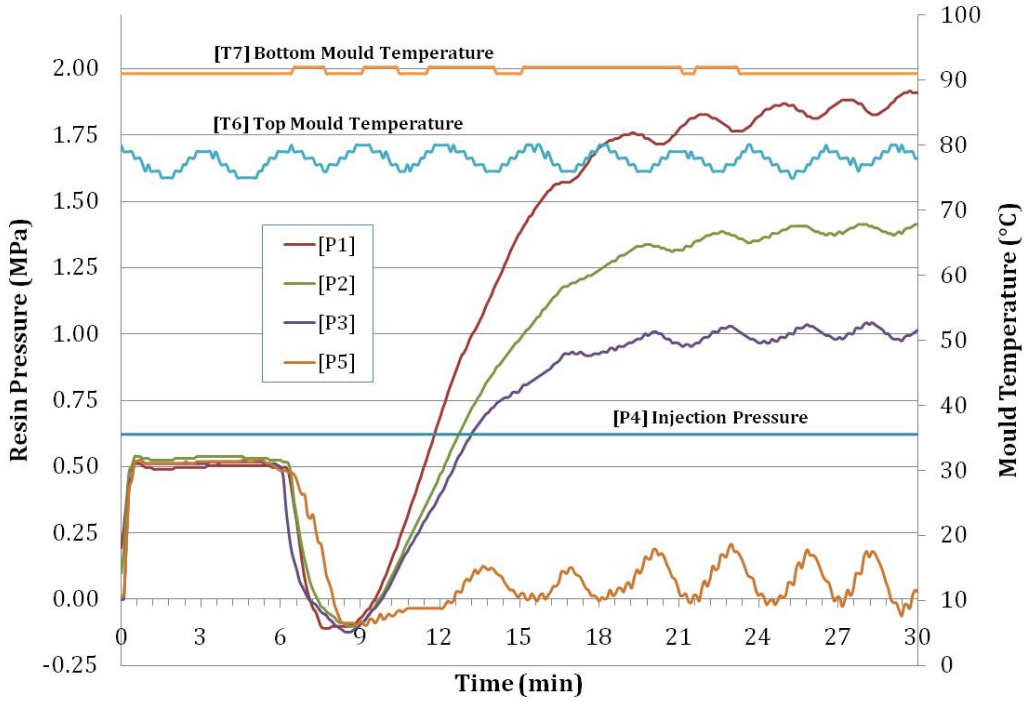

Figure 8.12: Pressure and temperature development during RTM injection #12 (test panel 5-1)

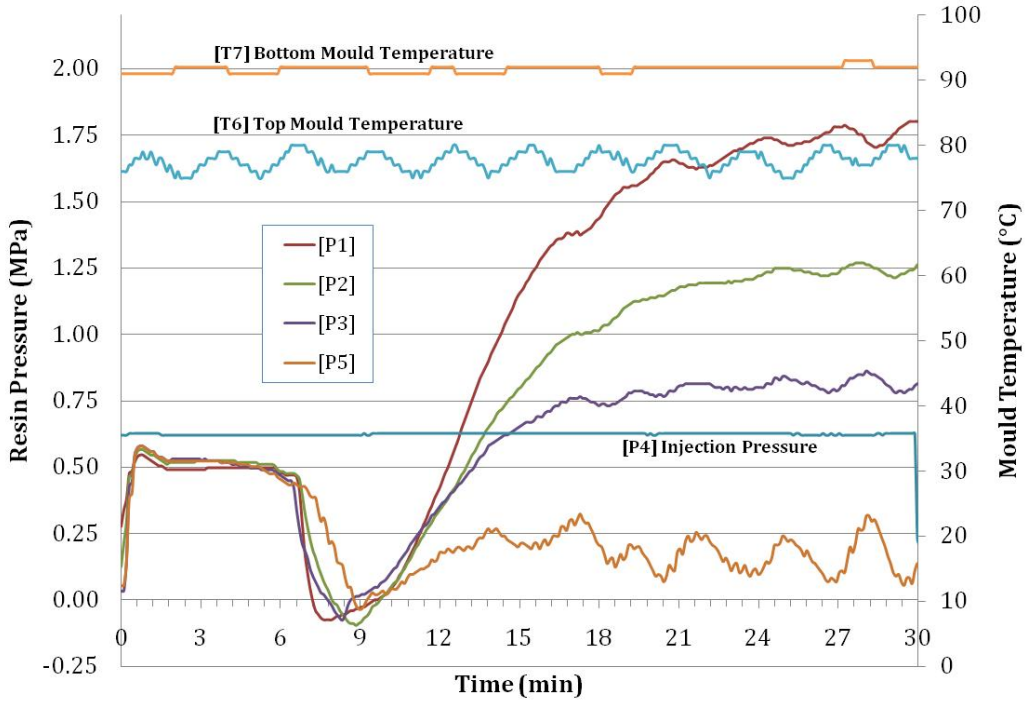

Figure 8.13: Pressure and temperature development during RTM injection #13 (test panel 8-1)

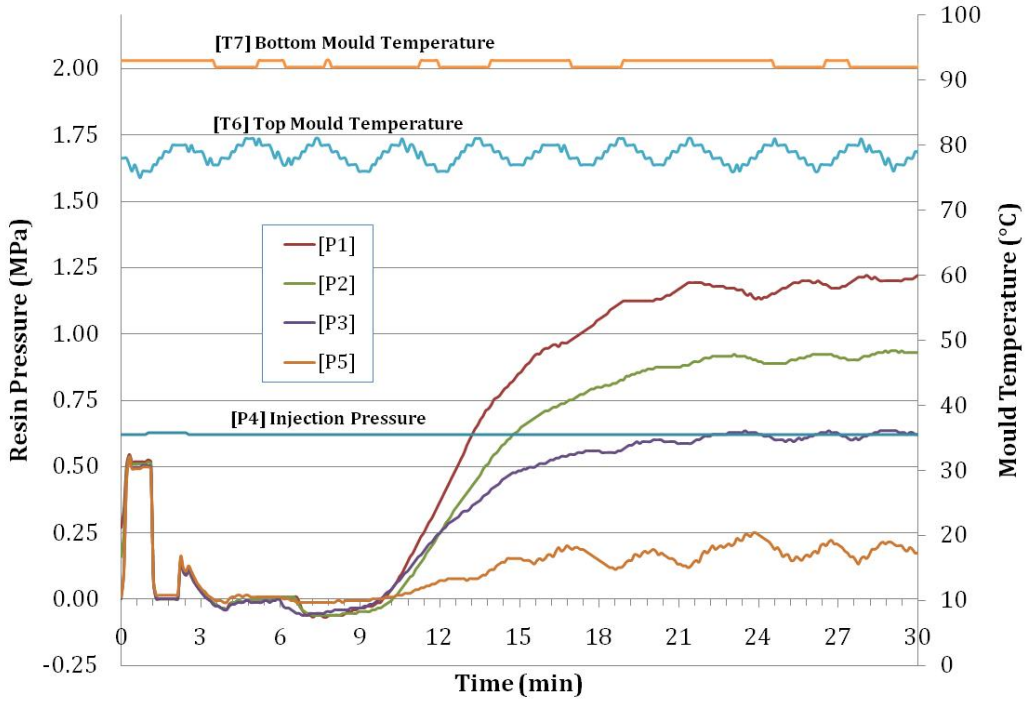

Figure 8.14: Pressure and temperature development during RTM injection #14 (test panel 4-2)

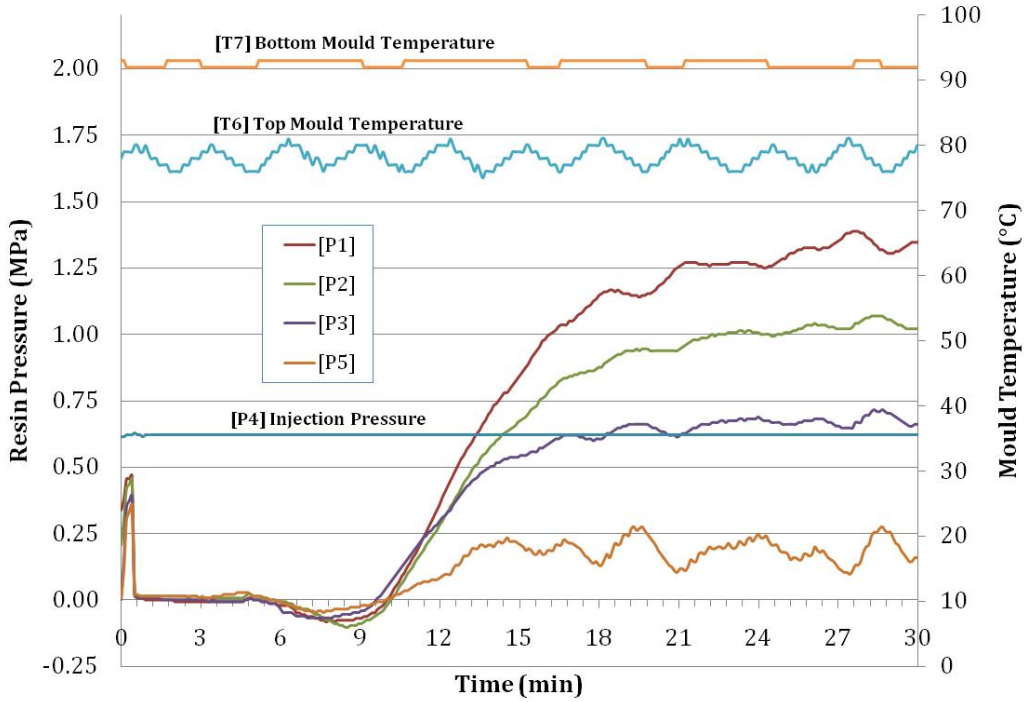

Figure 8.15: Pressure and temperature development during RTM injection #15 (test panel 2-2)

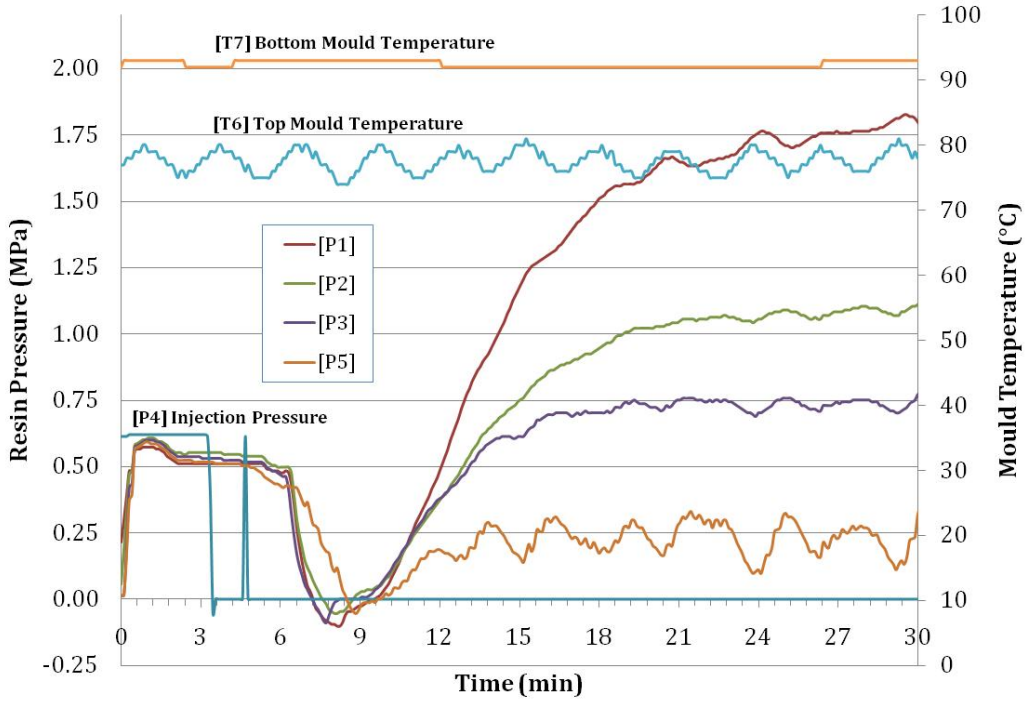

Figure 8.16: Pressure and temperature development during RTM injection #16 (test panel 6-2)

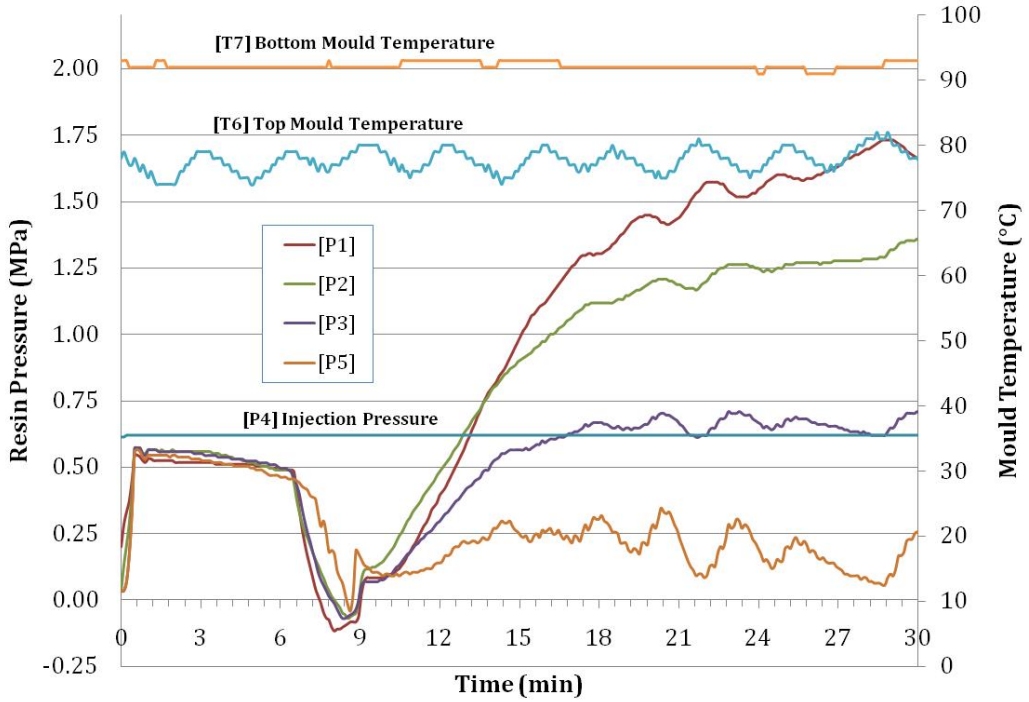

Figure 8.17: Pressure and temperature development during RTM injection #17 (test panel 8-2)

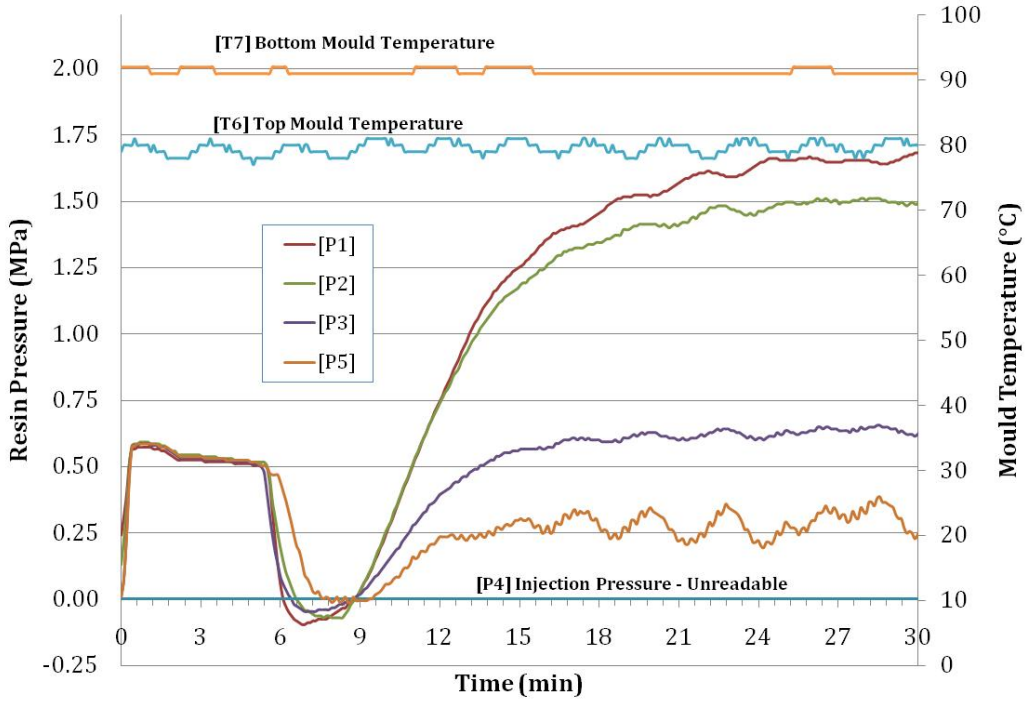

Figure 8.18: Pressure and temperature development during RTM injection #18 (test panel 5-2), note [P4] was unreadable due to a faulty connection

9 Appendix C

9.1 Dry Preform Imaging – Grayscale Roughness Results

Table 9.1: Average grayscale roughness values for each test panel

Name	Average Grayscale Roughness
1-1	8.3342
1-2	8.9296
2-1	9.8222
2-2	9.6468
3-1	8.2773
3-2	9.2395
4-1	9.4728
4-2	9.4695
5-1	9.1534
5-2	9.2090
6-1	8.4652
6-2	8.8573
7-1	9.4581
7-2	10.0503
8-2	8.9715
8-1	8.1516

9.2 Dry Preform Imaging – ANOVA Results

Table 9.2: Average grayscale roughness Mean-Squared Deviation results

Set #	Avg.	Std. Dev.	Range	MSD
1	8.632	0.421	0.595	74.6
2	9.735	0.124	0.175	94.77
3	8.758	0.68	0.962	76.94
4	9.471	0.002	0.003	89.7
5	9.181	0.039	0.056	84.3
6	8.661	0.277	0.392	75.06
7	9.754	0.419	0.592	95.23
8	8.562	0.58	0.82	73.47

9.3 ONDULO System – Average Roughness Results

Table 9.3: ONDULO average roughness values for each test panel

Name	Average Roughness	Max Reading	Min Reading
1-1	0.349	0.417	0.264
1-2	0.316	0.384	0.237
2-1	0.322	0.372	0.264
2-2	0.304	0.435	0.152
3-1	0.339	0.435	0.228
3-2	0.320	0.434	0.207
4-1	0.339	0.400	0.273
4-2	0.282	0.369	0.169
5-1	0.363	0.427	0.303
5-2	0.413	0.517	0.299
6-1	0.326	0.408	0.243
6-2	0.226	0.393	0.031
7-1	0.326	0.394	0.243
7-2	0.347	0.444	0.268
8-2	0.350	0.492	0.244
8-1	0.360	0.424	0.292

9.4 ONDULO System – ANOVA Results

Table 9.4: ONDULO average roughness Mean-Squared Deviation

Set #	Avg.	Std. Dev.	Range	MSD
1	0.332	0.023	0.033	0.111
2	0.313	0.012	0.018	0.098
3	0.33	0.014	0.019	0.109
4	0.31	0.04	0.057	0.097
5	0.388	0.035	0.05	0.151
6	0.276	0.071	0.101	0.079
7	0.336	0.015	0.021	0.113
8	0.355	0.007	0.01	0.126